G67-10569

X-571-67-532

C.1

FILE COPY

THE GODDARD RANGE AND RANGE RATE SYSTEM PERFORMANCE WHILE TRACKING IMP-F

G. C. KRONMILLER, JR.
D. J. ZILLIG

NOVEMBER 1967

GODDARD SPACE FLIGHT CENTER
GREENBELT, MARYLAND

PROPERTY OF
GODDARD SPACE FLIGHT CENTER
LIBRARY

LIBRARY
DEC 4 10 35 PM '67

X-571-67-532

THE GODDARD RANGE AND RANGE RATE SYSTEM

PERFORMANCE WHILE TRACKING IMP-F

G. C. Kronmiller, Jr.
D. J. Zillig

November 1967

GODDARD SPACE FLIGHT CENTER
Greenbelt, Maryland

CONTENTS

THE GODDARD RANGE AND RANGE RATE SYSTEM PERFORMANCE WHILE TRACKING IMP-F

I. INTRODUCTION

The IMP-F spacecraft was launched on May 24, 1967 into an orbit with an apogee of 211,000 km, a perigee of 265 km, and an inclination of 66.37°. The spacecraft was launched from the Western Test Range and the nominal sub-satellite plot is shown in Figure 1.

Tracking support for this type of an elliptical orbit was provided by the Goddard Range and Range Rate (GRARR) System using VHF equipment. GRARR sites are located at:

Rosman, N.C.
Tananarive, Malagasy Republic
Carnarvon, Australia
Santiago, Chile
Fairbanks, Alaska

The VHF transponder on IMP-F is a unified tracking, telemetry, and command system. Extensive documentation exists describing all aspects of the GRARR system. This document will describe the essential details of the VHF system, show the results obtained from each station while tracking IMP-F, and list pertinent system documents available to those readers desiring additional information about the GRARR system.

II. GRARR SYSTEM DESCRIPTION

The Goddard Range and Range Rate System determines spacecraft range, and range rate and angular position. The range measurement technique combines the advantages of harmonic and pseudo-random signals in a highly effective and versatile manner, operable either as an all-harmonic system in near-earth orbital tracking or as a hybrid system for tracking more distant spacecraft. The system also combines the utilization of the two types of signals in a very attractive technique for speeding up the process of acquiring the ambiguity resolving code component in tracking spacecraft at cislunar and translunar distances. Doppler techniques are employed to measure range rate and antenna position is employed to measure spacecraft angle.

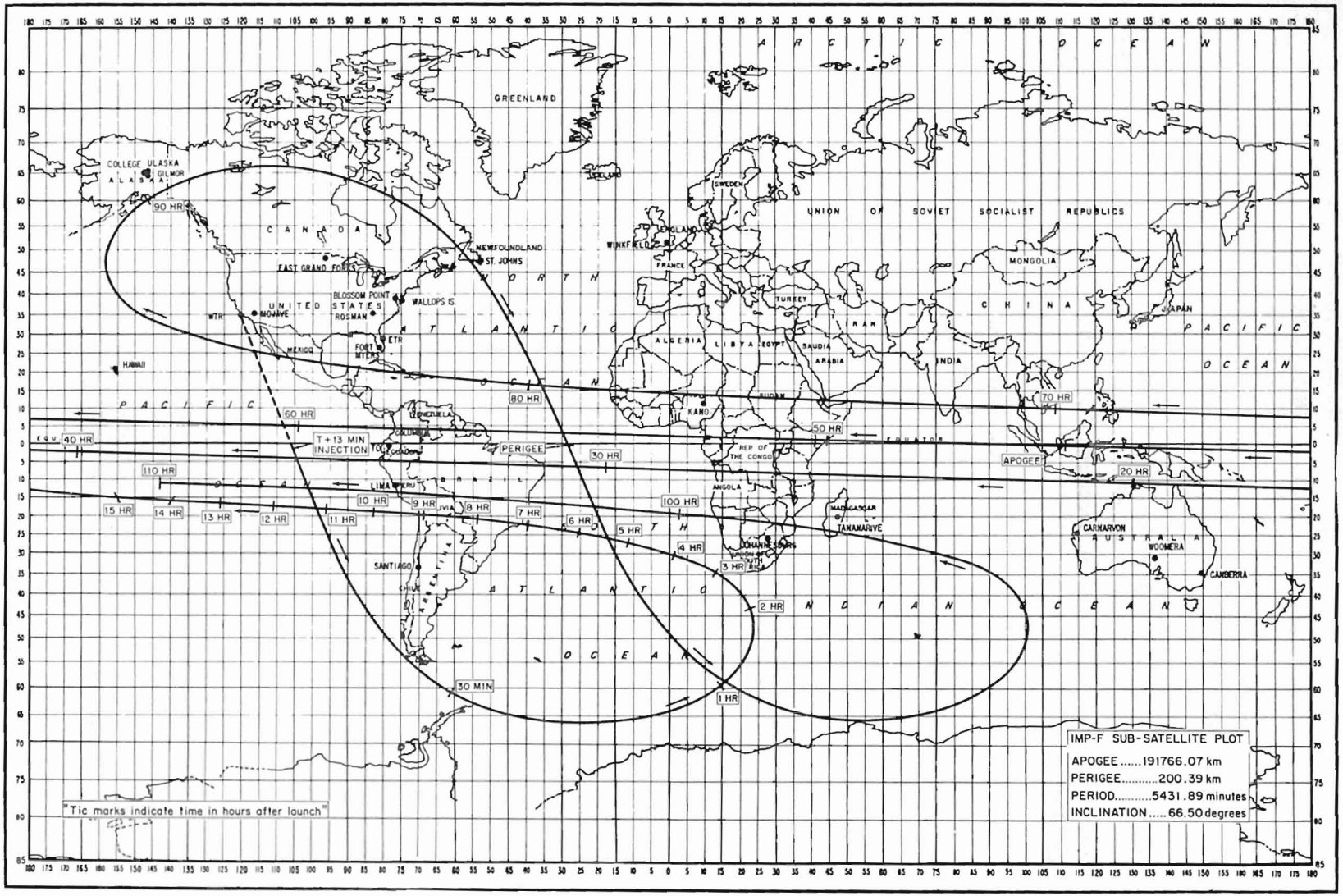
A R C T I C O C E A N
GREENLAND
ICELAND
COLLEGE ULASKA
ALASKA
GILMORE
90 HR
C A N A D A
NEWFOUNDLAND
ST. JOHNS
EAST GRAND FORKS
BLOSSOM POINT
ROSMAN
WALLOPS IS.
UNITED STATES
MOJAVE
WTR
ETR
FORT MYERS
MEXICO
HAWAII
P A C I F I C
O C E A N
60 HR
40 HR
EQU
T+13 MIN INJECTION
TOC
PERIGEE
110 HR
15 HR
14 HR
13 HR
12 HR
11 HR
10 HR
9 HR
8 HR
7 HR
6 HR
5 HR
4 HR
3 HR
2 HR
30 MIN
1 HR
30 HR
80 HR
100 HR
50 HR
70 HR
20 HR
APOGEE
EQUATOR
U N I O N O F S O V I E T S O C I A L I S T R E P U B L I C S
SWEDEN
ENGLAND
FRANCE
WINKFIELD
MONGOLIA
TURKEY
IRAN
C H I N A
JAPAN
ALGERIA
LIBYA
EGYPT
SAUDIA ARABIA
INDIA
KANO
REP OF THE CONGO
ANGOLA
MADAGASCAR
TANANARIVE
JOHANNESBURG
SOUTH AFRICA
CARNARVON
AUSTRALIA
WOOMERA
CANBERRA
LIMA
PERU
BRAZIL
SANTIAGO
CHILE
ARGENTINA
A T L A N T I C
O C E A N
I N D I A N O C E A N
"Tic marks indicate time in hours after launch"
IMP-F SUB-SATELLITE PLOT
APOGEE.....191766.07 km
PERIGEE.....200.39 km
PERIOD.....5431.89 minutes
INCLINATION.....66.50 degrees

Figure 1.

Overall System Description

A simplified block diagram of the GRARR system is shown in Figure 2. The system utilizes both S-band and VHF tracking equipment, however, this document will describe only the VHF portion.

In system operation, the VHF antenna sector scans around the expected spacecraft approach angle until the transponder carrier frequency is acquired by the VHF ground receiver. Then the antenna automatically reverts to an autotrack mode, range tones are applied to modulate the uplink VHF carrier and the VHF receiver starts extracting range, range rate, and angle data.

The sum of the ranging tones phase-modulates the uplink carrier. The transponder heterodynes the uplink signal in a double conversion process down to a pre-assigned sub-channel frequency space. The translated uplink carrier and range tones are then applied as phase modulation on the downlink carrier. Figure 3 shows the resultant spectra at the input and output of the VHF transponder. The frequency translation and retransmission are performed in such a manner that coherent two-way doppler measurements can be obtained by the ground station.

The VHF ground antenna is mounted on a hydraulically powered X-Y pedestal. The VHF antenna systems at Rosman, Carnarvon, and Tananarive consist of an array of cavity-backed slots mounted on a 28-foot square ground plane. They provide 20 db of gain at 148 MHz transmit frequency and 19 db at the 136 MHz receive frequency. The VHF antennas at Alaska and Santiago consist of a flat plate dipole array with 32 crossed dipole radiators arranged on a 28 square foot ground plane. They provide 20 db of gain at the 148 MHz transmit frequency and 21 db at the 136 MHz receive frequency. The outputs of the antenna elements are grouped and processed to generate one sum and two difference signals for phase-comparison monopulse angle tracking.

Associated with the antenna system is one sum-channel and two error-channel receivers. The sum-channel receiver contains the carrier and sub-carrier phase-locked loops. Its outputs consist of an AGC voltage and a reference signal for the error-channel receivers, a doppler plus bias signal for range rate extraction, and the demodulated range tones, ambiguity resolving code (ARC), and a rate-aiding signal for range extraction. The error-channel receivers provide synchronous amplitude detection of the X angle and Y angle tracking errors. The error signals drive a servo system that controls automatic angle tracking. A 16-bit angle encoder is used for precise angle read-out.

Range, range-rate and angle data are punched on paper tape, whence they are transmitted to GSFC via teletype in a format convenient for use in digital

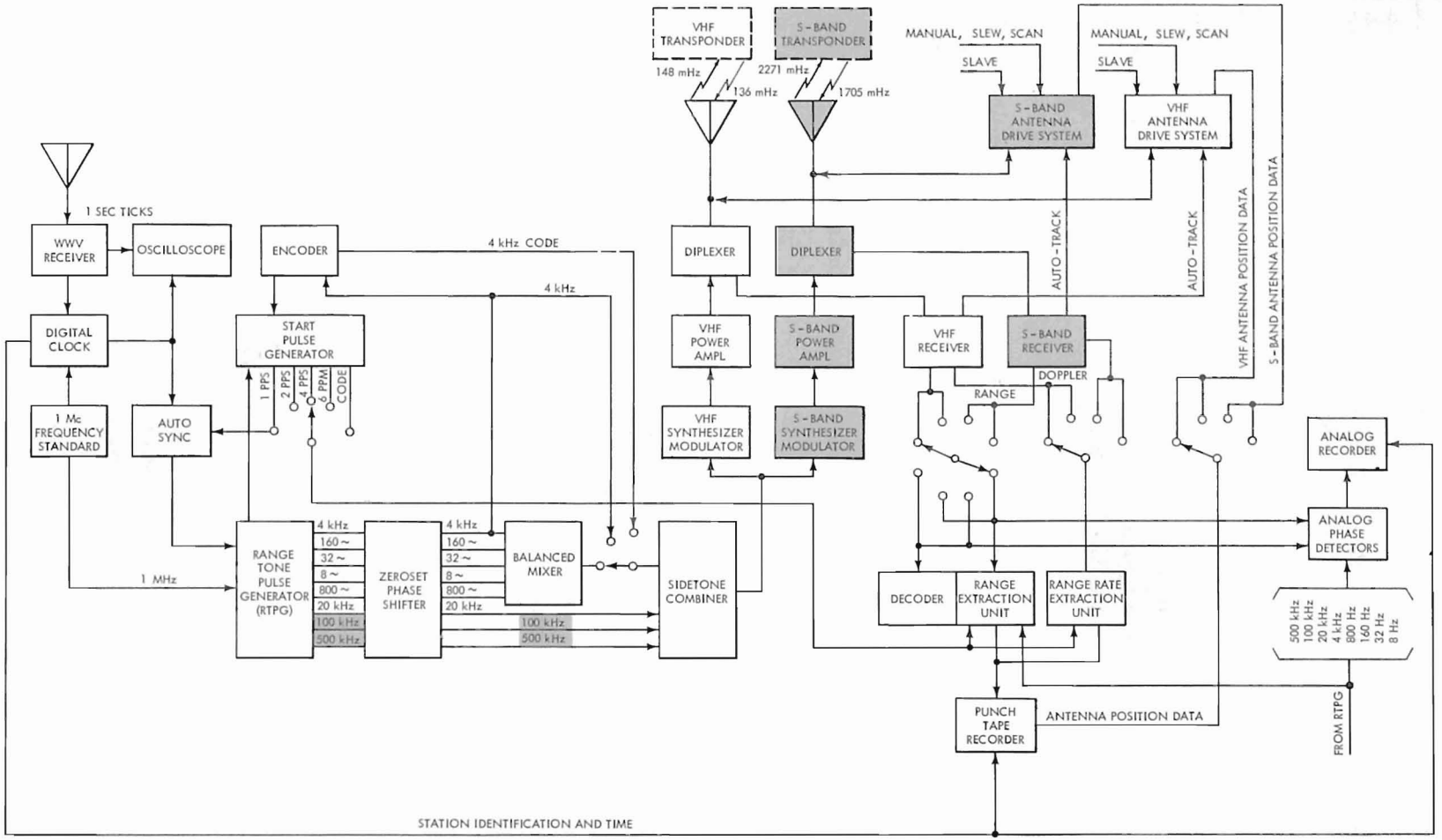

Figure 2. GRARR VHF System Block Diagram (S-Band System Shaded)

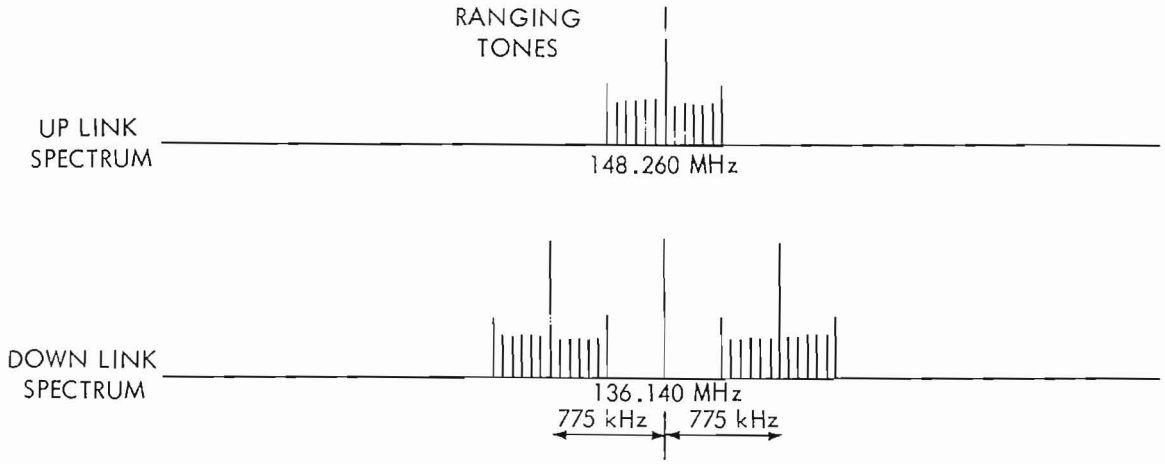

Figure 3. Spectra of VHF Transponder Input and Output Signals

computing facilities for rapid, precise calculation of the space vehicle orbital parameters.

The VHF system radiates 10 kw in its uplink signal. The power output is switchable to 1 kw for close-in tracking, if necessary, to avoid transponder saturation.

A 1 Mc frequency standard provides extremely stable reference frequencies for the entire system. The digital clock provides a local time standard from the frequency standard and provides a 1 pps output for time synchronization with WWV. The system time accuracy is thus essentially limited by the uncertainty in propagation time of the WWV signal. The timing equipment is chosen to be several orders of magnitude better than this propagation uncertainty in order to allow for improved system timing at a later date when a VLF WWV signal is made available with less propagation delay uncertainty.

Range Measurement (Sidetone)

Precision range measurements are accomplished by the use of ranging sidetones. The phase shift between ground-transmitted sidetones and transponder returned sidetones is directly proportional to the two-way range between the tracking antenna and the satellite. The ranging sidetone frequencies are 500 KHz, 100 KHz, 20 KHz, 4 KHz, 800 Hz, 160 Hz, 32 Hz and 8 Hz. Thus, except for the last tone, successive frequencies are in a 5:1 ratio. The highest frequency used in the VHF system is 20 KHz and is used to determine the finest

increment of range; the lower-frequency tones are used to resolve range measurement ambiguities.

The reference pulse generator is used to produce phase-coherent tones of 500 KHz, 100 KHz, 20 KHz down to 8 Hz. Reference pulses of 4 pps, 2 pps, 1 pps or 6 ppm are also generated. These tones and reference pulses are generated in a fully clocked digital divider chain using a 1 MHz frequency standard signal as an input. Thus, each of the reference pulses is coincident with positive-going zero crossings of the higher tones. A reference pulse (selected with the system data rate switch), along with a zero crossing of the 20 KHz tone is used to generate a start pulse that marks precisely the time of transmission of an all zero-phase condition for all the tones.

Prior to transmission, the ranging tones pass through the Zero-Set Phase Shifter Unit. This unit enables individual and combined phase shift of the ranging tones so that the individual transmitted tones can be phase-or time-shifted with respect to those used to generate the start pulse. In this way, an adjustable bias can be applied in the range time measurement to calibrate out the effect of fixed equipment time delays and differential time delays between tones.

The ground receiver uses an extracted carrier reference to shift the desired portion of the downlink RF spectrum down to a zero frequency center, filters the desired tones, and sends them to the Digital Range Tone Extractor. The Digital Range Tone Extractor regenerates clean tones that are phase coherent with the received tones in the following manner. The 20 KHz tone is used to drive a digital divide chain that regenerates all the other tones (i.e., 4 KHz down to 8 Hz). The reconstructed 4 KHz will be either in phase with the received 4 KHz or some multiple of 360/5 = 72 deg out of phase with it (i.e., 72 deg, 144 deg, 216 deg, 288 deg). The phases of the digitally generated 4 KHz and the received 4 KHz are compared, and the digitally generated 4 KHz is stepped in phase (by adding extra 20 KHz pulses) until a zero phase difference is indicated. Once the 4 KHz tone is locked, the 800 Hz tones are synchronized in the same manner. This same process is used to phase synchronize all of the digitally reconstructed tones.

The use of this digital tone extraction technique makes it possible to switch off lower-frequency tones (in the sidetone combiner) after acquisition, since only the highest tone is required to drive the digital divide chain.

Range Measurement (Hybrid)

A maximal-length sequence is employed for resolving ambiguities when the transit time to the spacecraft and back is greater than the period of the 8 cps

sidetone. The resulting hybrid system thus consists of the basic sidetone system modified to incorporate ambiguity resolution by a supplementary digital code ranging signal. Two independent range measurements are made, a tone range measurement and an ambiguity-resolving-code range measurement. The tone measurement uses tones from 20 KHz to 8 Hz, providing a precise range measurement that is ambiguous to an integral multiple of an 8 Hz half wavelength (i.e., an integral multiple of 18,750 km). The ambiguity-resolving-code signal is then used to resolve the 8 Hz ambiguities in the tone range measurement out to approximately 1,213,600 km.

The ambiguity-resolving (henceforth abbreviated AR) code used in the GRARR system is a linear combination of two relatively prime maximal-length subcodes whose lengths are 127 bits and 255 bits. The combination produces an output sequence that repeats every 32,385 bits and is driven at a clock rate of 4000 bits per second. This yields a code length of slightly over 8 seconds, corresponding to an unambiguous one-way range of 1,213,600 km.

The AR code is not applied until the tone system is completely acquired and tone ranging start and stop pulses are being generated. Once the tone system is acquired, the minor tones are removed from the transmitter and replaced with an AR-code-modulated 4 KHz subcarrier. The first tone start pulse is used by the AR Decoder Control logic to simultaneously stop the AR Decoder and set its register contents equal to the contents of the transmitter AR Encoder. When the tone stop pulse is received by the control logic, the AR Decoder is started, using the doppler shifted 4 KHz from the Digital Range Tone Extractor as a clock. Thus, the AR Decoder has been offset in time from the AR Encoder by the ambiguous two-way transit time to the spacecraft, as measured by the tone system. The AR Decoder will then be either in phase with the received demodulated code, or time-shifted from it by an integral number of 1/8 second (500-bit) intervals. The acquisition process now consists of making a trial correlation between the AR Decoder and the received AR code and if correlation is not indicated, stepping the AR Decoder by 500 bits (1/8 sec) and testing again for correlation. This process is repeated until correlation is achieved. The Ambiguity Number Counter receives a pulse from the decoder logic circuit each time the AR Decoder is stepped 500 bits, keeping track of the number of 8 Hz periods involved. A set of thumbwheel digiswitches also enables the operator to start the acquisition sequence at any range ambiguity slot, allowing maximum use to be made of any a priori range information.

After correlation has been achieved and the hybrid system is completely phase-locked to the returned signal, the number in the Ambiguity Number Counter indicates the number of full 1/8 sec periods in the round-trip time to the spacecraft. The hybrid system now provides a continuous periodic check

on this number so that it will automatically be updated when the spacecraft range changes to a new ambiguity slot.

Transponders

VHF Transponder—The functional block diagram of the VHF transponder is shown in Figure 4. The incoming signal is heterodyned down to a pre-assigned subcarrier frequency by mixing with a multiple of a locally generated reference signal. The reference oscillator frequency, f_0 (22.690 MHz), is used in a double conversion to translate a signal of uplink received carrier frequency $f_{up} + f_{up,d}$ to a subcarrier at $f_{up} + f_{up,d} - 6.5\, f_0$. The subcarrier is used to phase modulate the downlink carrier. It should be noted that the transponder transmitter frequency is derived from the reference oscillator, f_0, which was used to generate the LO frequencies for the double conversion to the subcarrier. This technique enables the downlink signal to be usable by the ground stations to extract two-way doppler for range rate measurement, free of the effects of the transponder reference oscillator instabilities, and without requiring separate telemetered information about spacecraft oscillators.

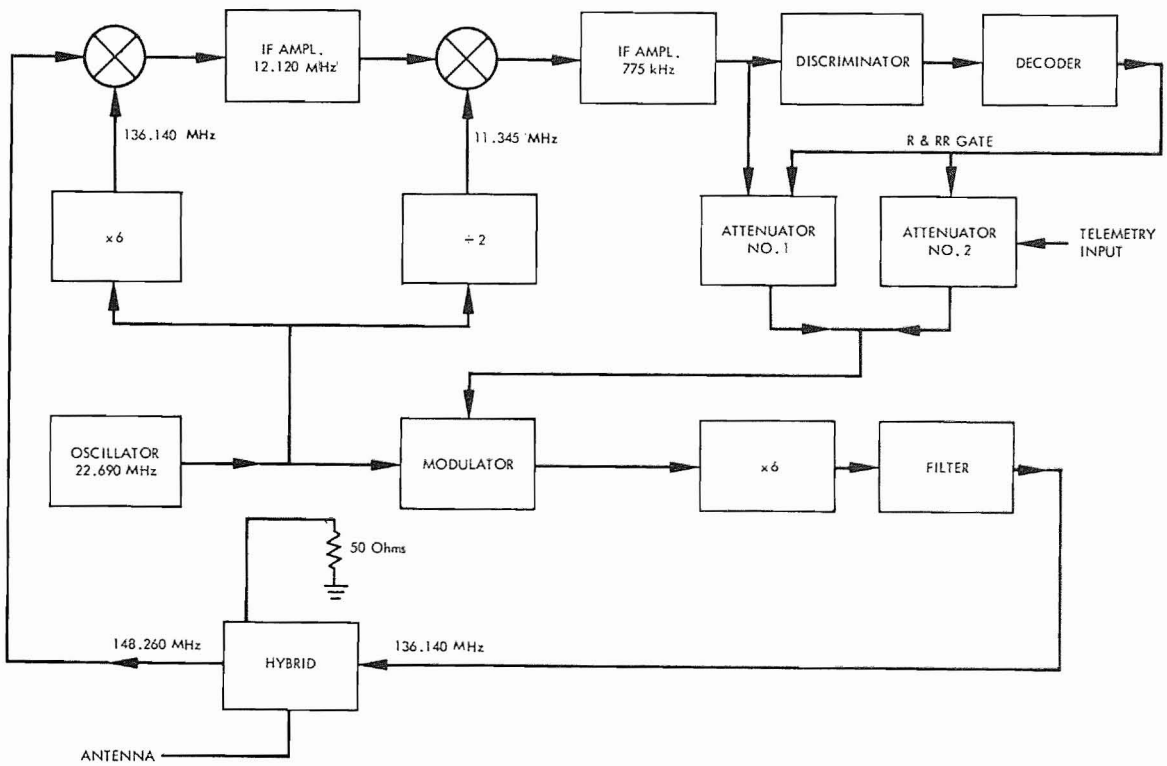

Figure 4. VHF Transponder

The VHF transponder also serves as a telemetry transmitter for the spacecraft. The ranging function is energized by a command tone that allows the ranging modulation to be placed on the carrier. Thereafter, the presence of the 4 KHz ranging tone holds the transponder in the ranging condition until the tones are turned off, at which time the transponder reverts back to a simple telemetry transmitter.

The design specifications of the VHF transponder are given in Table I.

Table I

Design Specifications of GRARR VHF Transponder

Input Signal Level	-50 to -115 dbm
Input Frequency	148.260 MHz
Channel Frequency	775 KHz
Multiplication Ratio (transmit/receive)	12/13
Channel Information Bandwidth	60 KHz
Maximum One-Way Doppler Shift	±5 KHz
Transmitted Carrier Frequency	136.140 MHz
Transmitted Power	4 watts
Transponder Group Delay	17 μsec
Noise Figure	8 db

Range Rate Measurement

Range rate is determined from the two-way doppler shift of the uplink carrier frequency. In order to measure this doppler shift, it is necessary to maintain coherence of the uplink frequency through the transponder and back to the ground receiver where it is compared in frequency against a continuing sample of the uplink frequency in the range rate extraction unit. The range rate extraction unit measures doppler by counting a preset number of cycles of the sum of the doppler shift plus a known frequency offset, and determines the elapsed time through a time interval unit.

The uplink carrier is generated from an ultra stable 4.94 MHz crystal oscillator. By starting at approximately 5 MHz, as opposed to a higher frequency, better short-term stability can be achieved. This 5 MHz signal is frequency multiplied by 30 to produce a VHF frequency, f_{up}. This signal is amplified, and radiated to the transponder, arriving as $f_{up} + f_{up,d}$ where $f_{up,d}$ is the one-way doppler on f_{up} resulting from the transponder range rate $\dot{r}$ and is given very approximately by

$$f_{up,d} = (\dot{r}/c) f_{up} , \quad \text{for} \quad |\dot{r}/c| << 1$$

The received signal is processed by the transponder, as described previously, to generate a subcarrier ($f_{up} + f_{up,d} - 6.5\ f_0$) which is then used to phase-modulate a 6.0 f_0 downlink carrier. This signal is transmitted down to the ground receiver where it is received with a doppler shift because of transponder motion relative to the tracking station. The signal at the ground receiver has a carrier frequency of 6.0 ($f_0 + f_{0,d}$) and a subcarrier frequency of $\left[f_{up} + 2f_{up,d} - 6.5\ (f_0 + f_{0,d})\right]$ corresponding to an original uplink frequency f_{up}. The objective of the ground receiver and doppler extractor circuit is to extract the $2f_{up,d}$ term, the coherent two-way doppler on f_{up}.

The receiver carrier loop locks a VCO to the incoming carrier providing a reference at $f_0 + f_{0,d}$. The carrier loop "phase detector" also yields the subcarrier. The subcarrier loop phase locks a VCO to this subcarrier, producing a reference signal at $\left[f_{up} + 2f_{up,d} - 6.5\ (f_0 + f_{0,d})\right]$. The doppler extractor takes these two signals, along with the transmitter reference $f_{up}/6$ and combines them to produce $\left[30\ \text{KHz} + 2f_{up,d}\right]$. Thus, the desired $2f_{up,d}$ term has been obtained on a bias frequency of 30 KHz. This doppler extraction process therefore tends to cancel out any instability or jitter on the transponder oscillator, f_0, provided that these instabilities are properly tracked by both carrier and subcarrier phase-locked loops.

The range rate extraction unit measures the time interval associated with N_0 cycles of the bias plus doppler signal. When a reference pulse is received, a start pulse is generated to start the time interval unit counting 10 MHz pulses. The start pulse also starts gating in cycles of bias plus doppler to the N_0-cycle counter. When N_0 cycles have been counted, a stop pulse is generated to stop the time interval unit. The count of 10 MHz cycles in the time interval unit can be expressed as

$$N = \frac{N_0 \times 10^7}{\left(f_b + 2f_{up,d}\right)}$$

This count is made available to the Data Multiplexer in eight BCD decades (32 parallel lines). The two-way doppler can then be computed from a knowledge of N, the N_0 used and the bias frequency f_b.

III. GRARR SIGNAL CHARACTERISTICS

The GRARR system transmits range tones, a range ambiguity resolving code and tone commands to the IMP-F spacecraft. The range tones are fixed

by system design to be 20 KHz, 4 KHz, 800 Hz, 160 Hz, 32 Hz and 8 Hz. All range tones below 4 KHz are transmitted as upper sidebands of the 4 KHz tone. The tones may be sent in either parallel mode (all tones simultaneously) or sequential mode (two at a time). The sequential mode applies only to Alaska and Santiago. The ambiguity resolving code is a pseudo random sequence of 32,385 bits having a 4 KHz bit rate and is bi-phase modulated on the 4 KHz range tone. The tone commands consist of an address and three execute tones, all less than 4 KHz, sent in programmed sequence.

The transponder on board the IMP-F spacecraft was designed to share the transponder power with the telemetry system during the ranging operation. When the spacecraft is in the ranging mode, following the ranging command, the modulation index of the GRARR signal is 0.7 radian and the telemetry is 0.3 radian. Thus over most of the orbit, telemetry can still be received while the ranging process is taking place.

The GRARR earth-to-space spectrum is dependent only on the type of signal to be sent. The modulation indices for each type signal have been chosen for overall system performance and are fixed. The GRARR modulation indices for IMP-F are shown in Table II.

Table II

GRARR Earth-to-Space Modulation Indices (Radians Peak)

Signal Component	Ranging Operation	
	Parallel	Sequential
Major Tone (20 KHz)	0.7	0.7
Minor Tones*	0.2	0.7
Code**	0.45	0.7
	Command Operation	
Address Tone	1.0	
Execute Tone	1.0	

*Minor tones are 4 KHz, 4.008 KHz, 4.032 KHz, 4.160 KHz and 4.800 KHz.

**The modulation index of the code in radians RMS is determined by the modulation index of the 4-KHz tone (code carrier) in radians peak.

When the uplink modulation indices listed in Table II are employed, the relative sideband levels of the earth-to-space spectrum shown in Table III and Figures 5 and 6 result.

Table III

Relative Sideband Amplitude GRARR Earth-to-Space Spectrum

Signal Component	Mode of Operation			
	Parallel		Sequential	
	Ref to Unmod Carrier	Ref to Mod Carrier	Ref to Unmod Carrier	Ref to Mod Carrier
Carrier	-1.5 db	0.0 db	-2.3 db	0.0 db
Major Tone	-10.0 db	-8.5 db	-10.8 db	-8.5 db
Minor Tone	-21.5 db	-20.0 db	-10.8 db	-8.5 db
Code*	-14.1 db	-12.6 db	-10.8 db	-8.5 db

*The levels listed for the code are actually for that of the 4-KHz tone without code modulation.

Space-to-Earth Spectrum

The IMP-F transponder modulation index for GRARR is 0.7 radian peak. The space-to-earth relative sideband levels for IMP-F are presented in Table IV and the space-to-earth spectra, parallel and sequential modes, are presented in Figures 7 and 8.

Space-to-Earth Parameters

The space-to-earth parameters for IMP-F spacecraft are shown in Table V the operating margin for the system is designated in Table VI.

In Table V, it is seen that the sum of transponder power plus ground antenna gain less miscellaneous and other losses is 35.7 db, 43.7 db and 53.7 db for the minimum, probable and maximum cases, respectively. The algebraic sum of the above gain and the free-space attenuation at 210,000 km yields minimum,

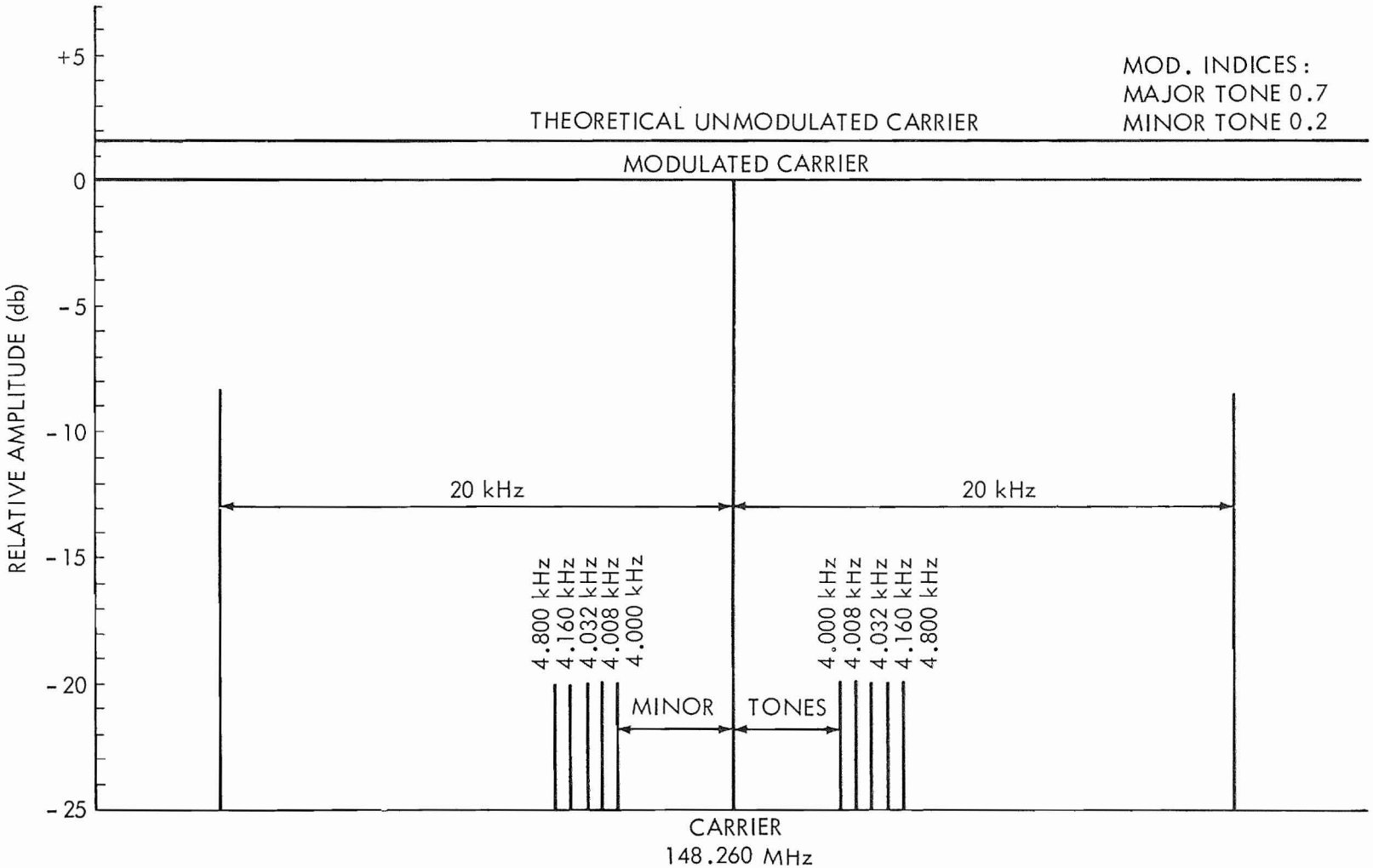

Figure 5. IMP-F Uplink Spectrum (Parallel Mode)

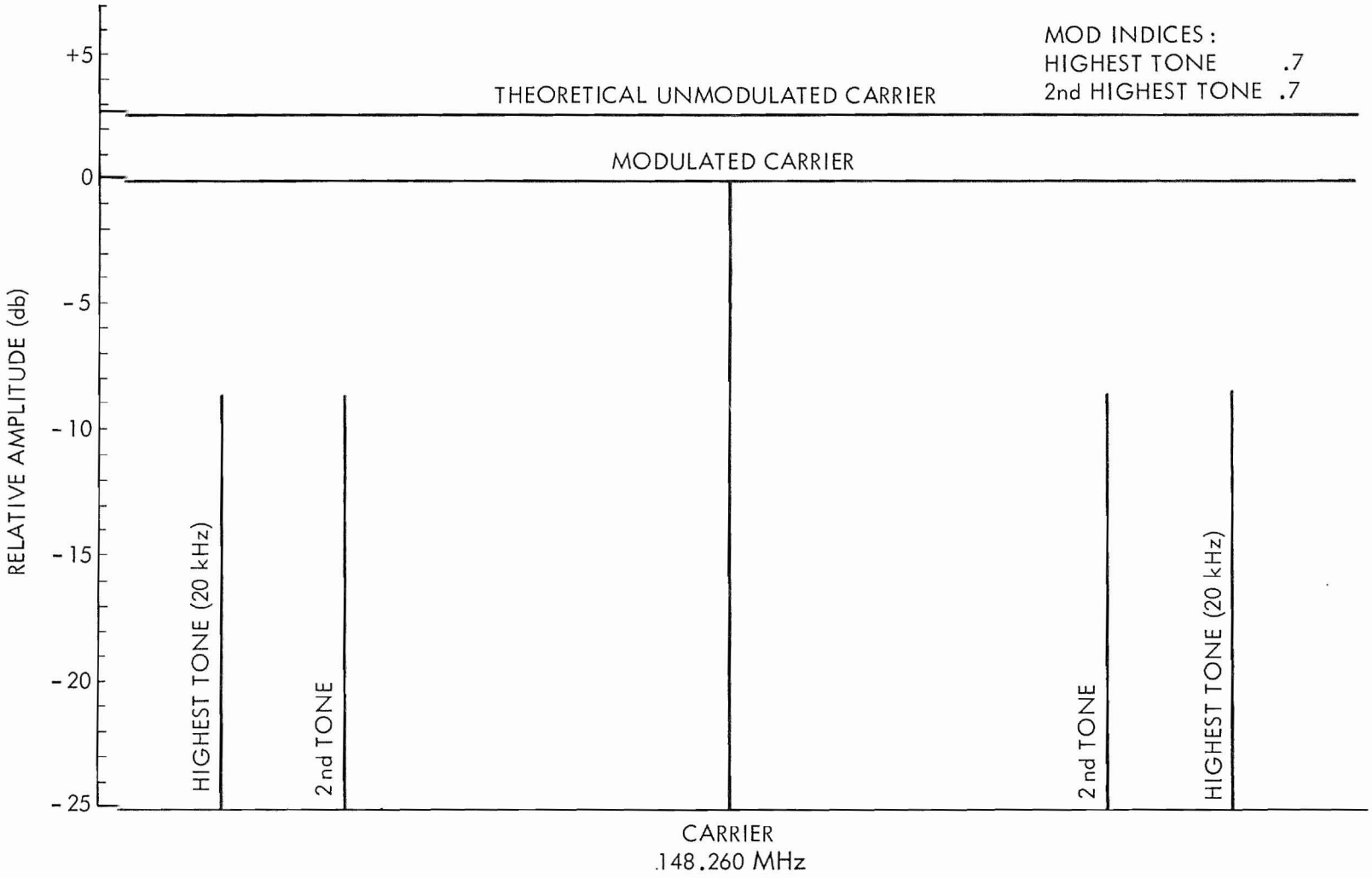

Figure 6. IMP-F Uplink Spectrum (Sequential Mode)

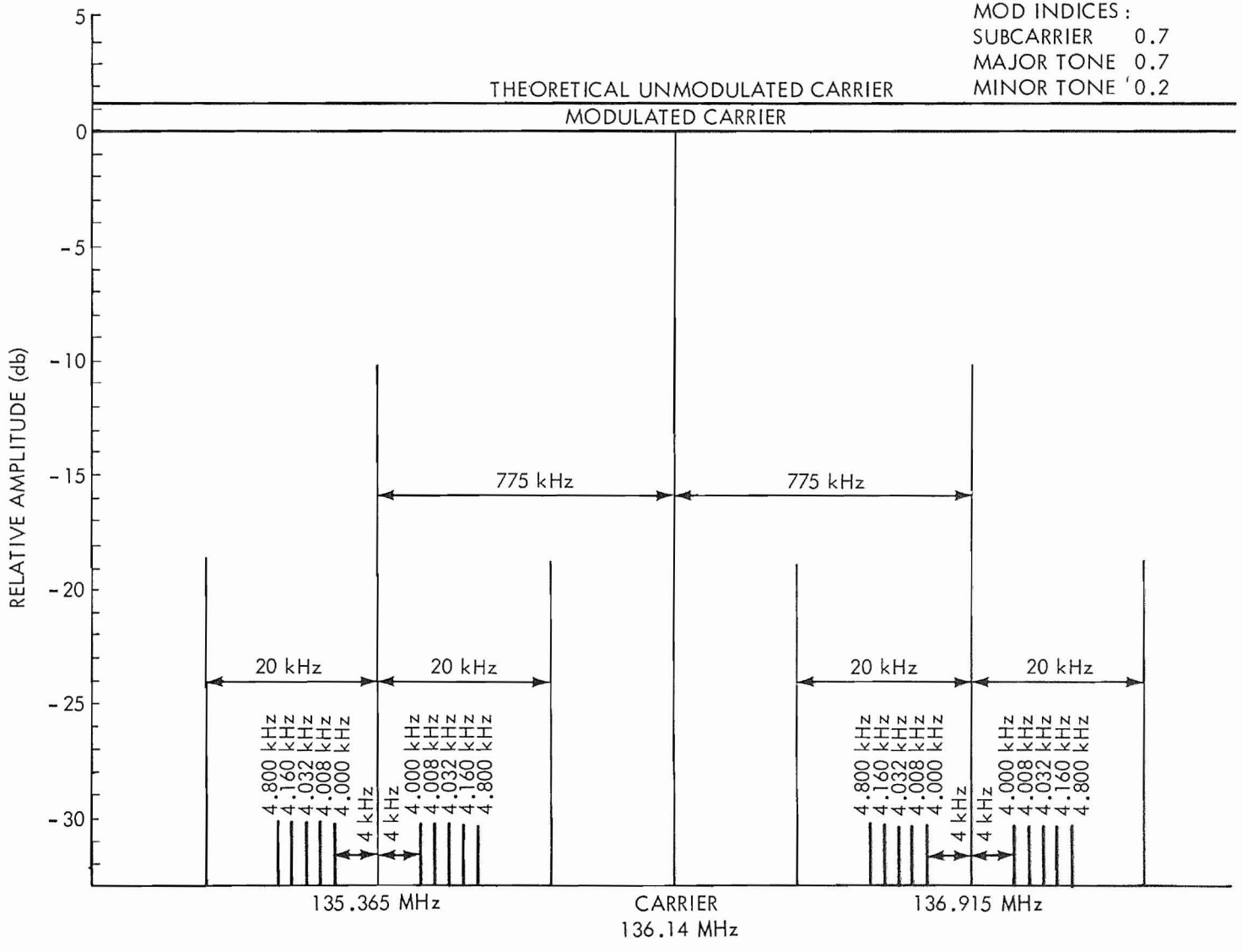

Figure 7. IMP-F Downlink Spectrum (Parallel Mode)

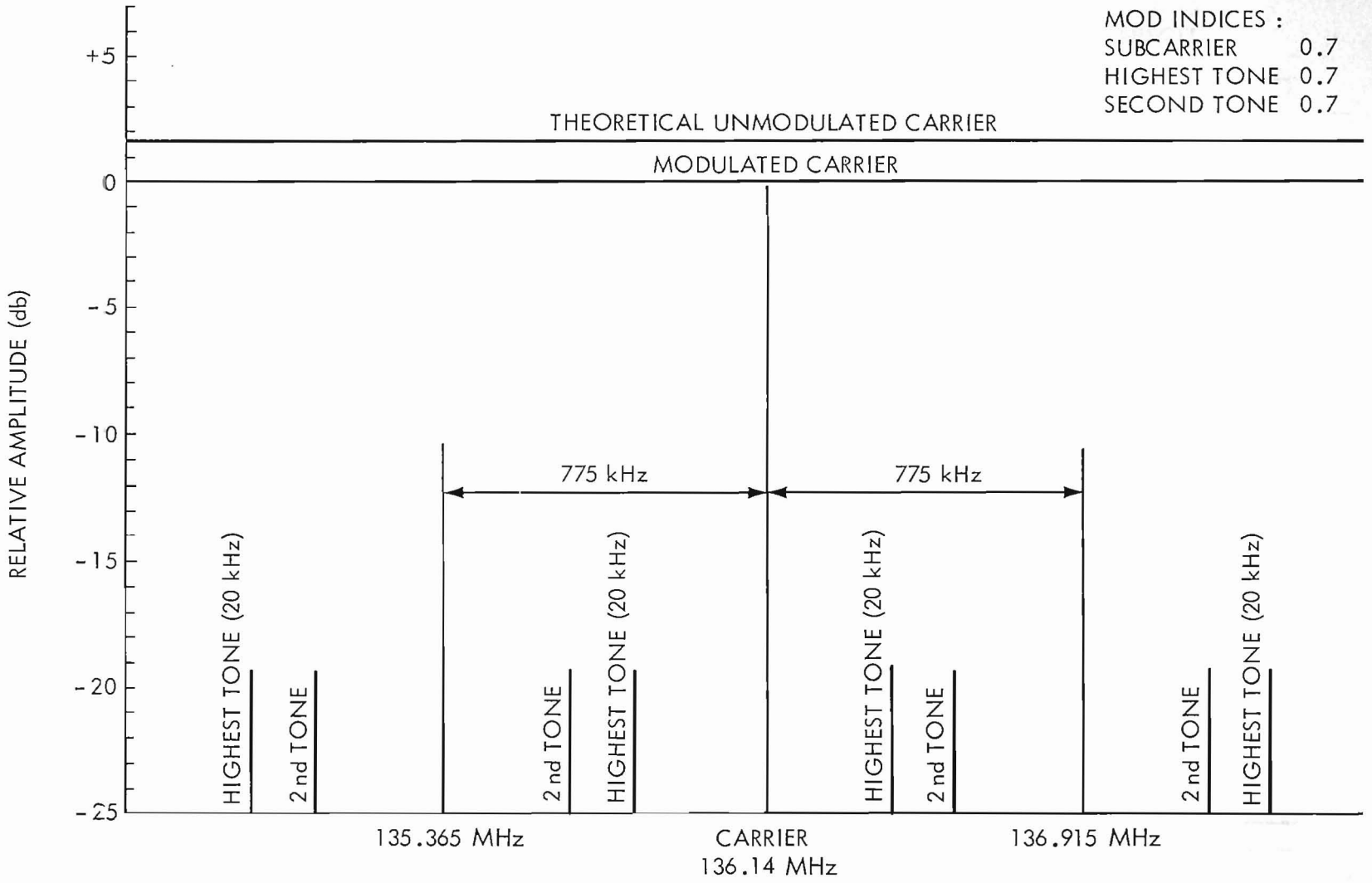

Figure 8. IMP-F Downlink Spectrum (Sequential Mode)

Table IV

Relative Sideband Amplitude GRARR Space-to-Earth Spectrum

Component	Mode of Operation			
	Parallel		Sequential	
	Refer to Unmod Carrier	Refer to Mod Carrier	Refer to Unmod Carrier	Refer to Mod Carrier
Mod Carrier	-1.3 db	-0.0 db	-1.3 db	0.0 db
Subcarrier	-11.4 db	-10.1 db	-12.2 db	-10.9 db
Major Tone	-19.9 db	-18.6 db	-	-
Minor Tone	-31.4 db	-30.1 db	-	-
Highest Tone	-	-	-20.7 db	-19.4 db
2nd Tone or Code	-	-	-20.7 db	-19.4 db

Table V

IMP-F Space-to-Earth Parameters

	Minimum	Probable	Maximum
Transmitted Power	36.0 dbm	36.0 dbm	36.0 dbm
Modulated Carrier Loss	-1.3 db	-1.3 db	-1.3 db
Spacecraft Antenna Gain	-6.0 db	-4.0 db	0.0 db
Polarization Loss	-6.0 db	-3.0 db	0.0 db
Ground Antenna Gain	19.0 db	19.0 db	19.0 db
Miscellaneous Losses	-6.0 db	-3.0 db	0.0 db
Propagation Loss (210,000 km)	-181.5 db	-181.5 db	-181.5 db
Expected Carrier Power* (210,000 km)	-145.8 dbm	-137.8 dbm	-127.8 dbm

*Measured at input to pre-amplifier.

Table VI

IMP-F System Operating Margin

Station	Best Possible	Average Expected	Worst Expected
Rosman, Tananarive Carnarvon	+27.2 db	+17.2 db	+9.2 db
Santiago, Alaska	+29.2 db	+19.2 db	+11.2 db

probable and maximum expected carrier power levels of -145.8 dbm, -137.8 dbm and -127.8 dbm, respectively.

The system operating margin is determined by subtracting the value of the system carrier threshold from the expected carrier power level. The system carrier threshold at Rosman, Tananarive and Carnarvon is -155 dbm; the system carrier threshold at Alaska and Santiago is -157 dbm.

Received Signal Levels (Expected Carrier Power Levels)

Received signal levels for IMP-F spacecraft are indicated in Figure 9 and Table VII.

Table VII

IMP-F Received Signal Levels

Range (km x 10^3)	Free Space Attenuation (db)	Theoretical Signal Level (dbm)		
		Minimum	Probable	Maximum
0.2	121.1	-85.4	-77.4	-67.4
1	135.1	-99.4	-91.4	-81.4
2	141.1	-105.4	-97.4	-87.4
5	149.1	-113.4	-105.4	-95.4
50	169.1	-133.4	-125.4	-115.4
100	175.1	-139.4	-131.4	-121.4
150	179.1	-143.4	-135.4	-125.4
200	181.1	-145.4	-137.4	-127.4

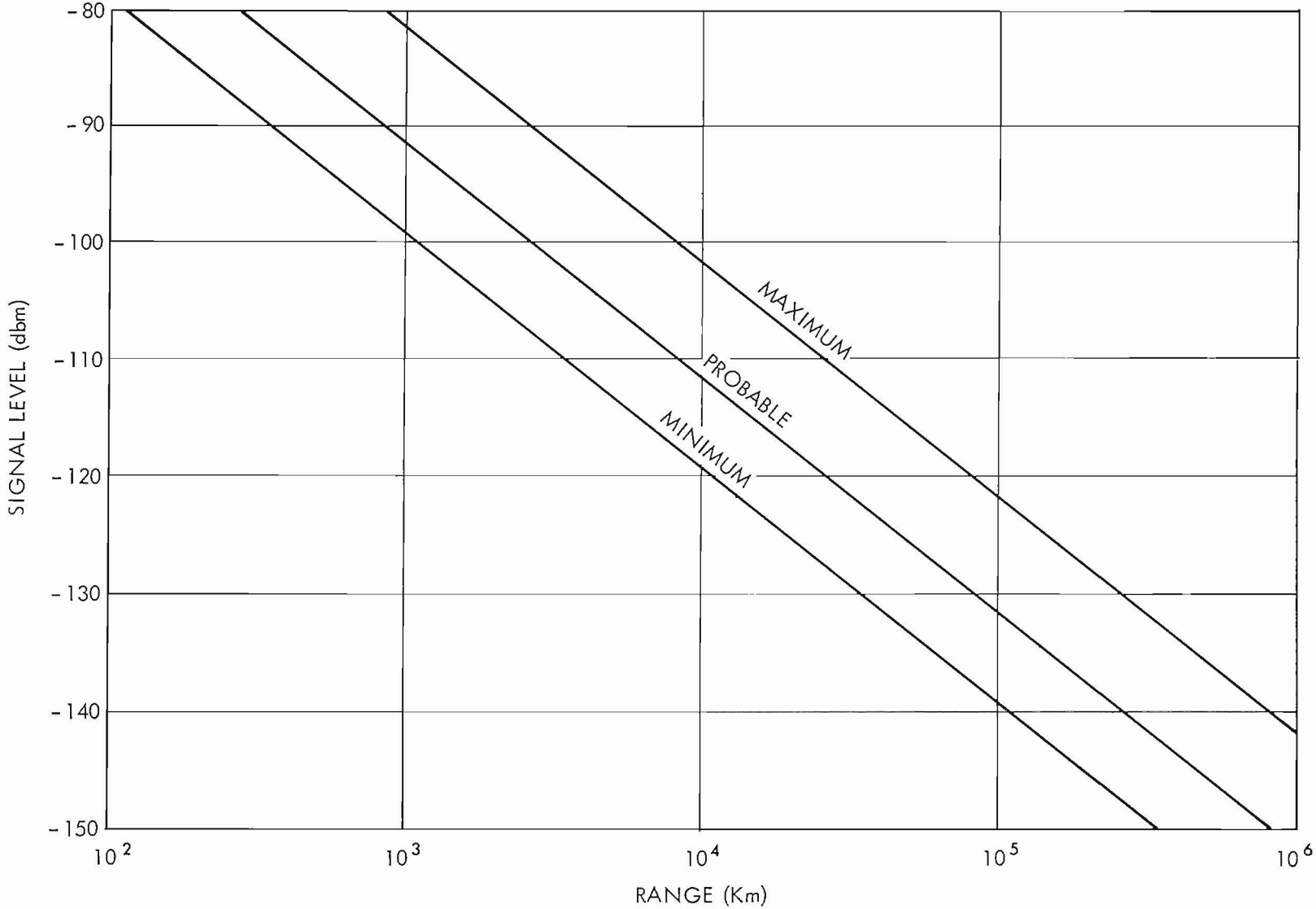

Figure 9. Signal Level versus Range (IMP-F Downlink)

IV. IMP-F TRACKING DATA

A complete description of all the processes the data are subjected to before being used in the orbital computation or a description of the orbital computation is beyond the scope of this document. A brief description of how the data get from the tracking station to the computer is included as a prelude to the graphs which present the actual results from the computer processing.

Data were gathered for ten minutes at spaced intervals around the IMP-F orbit. The data sampling rate was one sample per second resulting in a possible 600 data samples for each track from each station. These data were sent to GSFC via teletype and recorded on a punched paper tape. The teletype tape was then read into a CDC-160A computer where the data are corrected for WWV propagation time to the various sites, smoothed by a polynomial equation in groups of 32 points and re-formated, with one point representing each smoothed group, on magnetic tape for use in a 7094 computer.

Another processing route is sometimes used in which the CDC-160A places the raw data (corrected only for teletype garbles and data flagged as questionable) directly on magnetic tape. A program in the 7094 then process the data in blocks of 96 points. This processing corrects the data for WWV propagation time, smoothes the data with a polynomial equation, provides a smoothed data point for further orbit computation and computes an RMS range error and RMS range rate error for the data. The output of this program was used to obtain the RMS error values for the graphs in this report.

The smoothed and corrected data are then used in the 7094 which performs the orbital computation. The computer computes the orbital parameters and computes a data point (c) which is compared with the observed data point (o) and expressed as a value o-c. A process of differential correction and successive iterations of the orbit computation are performed in an effort to minimize all of the values of o-c. When the computer process converges to a solution where the o-c's remain fairly constant, a best fit to the data set is considered to have been reached and the process is stopped. The data presented in this report are the final values for the IMP-F orbits considered.

Using the computer processed data which provided RMS range errors, RMS range rate errors, orbital o-c values and daily status reports from each site which provided signal level and approximate values of spacecraft range, seven graphs were prepared for each site. The data were gathered for the periods May 24 to June 24, 1967 and July 1 to 15, 1967. This was done because, during the early orbit period, the spacecraft's perigee was low enough to experience a significant drag effect. In the later orbit period, perigee had increased out of the drag region and more accurate orbital computations resulted.

The seven graphs are:

May 24—June 24, 1967

1. Signal level vs Range
2. RMS Range error vs Range
3. RMS Range Rate error vs Range
4a. Range o-c vs Range
5a. Range Rate o-c vs Range

July 1-15, 1967

4b. Range o-c vs Range
5b. Range Rate o-c vs Range

The abscissa of each graph is range. Each vertical line represents the maximum variation of the ordinate at the mean range of the pass. While each line ideally represents the variation during one pass, the plotting of several passes at the same or nearly the same ranges has caused some overlap.

The GRARR system, as any operational system, is subject to problems such as signal interference, equipment failures, signal fading, and operator errors which result in poor data. No attempt has been made to select only the best data to present in the graphs because the authors wanted this report to show actual system performance. A portion of the range and range rate RMS error data and o-c data was found to be so grossly in error as to make it unfeasible to be included in the graphs. Where this occurred, a reasonable cutoff value was selected and only data equal to or below this value were plotted. Table VIII lists the cutoff values selected and the percentage of the data which is included in the graphs.

Explanation of the Graphs

1. Signal Level vs Range

The receiver AGC variation in dbm is plotted vs a mean value of range for the pass. The graph also contains the theoretical maximum, probable, and minimum signal level vs range plots for IMP-F as determined from Tables V and VII and illustrated in Figure 9.

2. RMS Range Error vs Range

The range error variation in meters RMS is plotted vs a mean value of range for the pass. RMS range errors are caused by noise on the 20 KHz range

Table VIII

Percentage of Data Below Cutoff Value

	May 24—June 24, 1967				July 1-15, 1967	
	Range Error	R Error	Range o-c	R o-c	Range o-c	R o-c
Cutoff Value	250 Meters	1.4 Meters/sec	3000 Meters	1.4 Meters/sec	3000 Meters	1.4 Meters/sec
Rosman	81%	99%	89%	93%	86%	92%
Tananarive	85%	95%	58%	82%	74%	97%
Carnarvon	72%	43%	72%	51%	70%	96%
Santiago	98%	100%	90%	88%	96%	93%
Alaska	98%	99%	88%	83%	100%	99%

tone used for range measurement with the main contributions coming from receiver excess noise, antenna noise, galactic noise and also oscillator noise associated with the phase-lock loop. A minimum expected system performance curve is also plotted.

3. RMS Range Rate Error vs Range

The Range rate error variation in meters per second RMS is plotted vs a mean value of range for the pass. The RMS range rate errors are caused by phase noise resulting from thermal noise on the Doppler signal, noncoherent oscillator noise, and cycle counting quantization noise. A minimum expected system performance curve is also presented.

4a,b. Range o-c vs Range

The range o-c variation in meters is plotted vs a mean value of range for the pass. Plots are made for range o-c vs range for the time periods (a) May 24—June 24, 1967 and (b) July 1-15, 1967.

5a,b. Range Rate o-c vs Range

The range rate o-c variation in meters/second is plotted vs a mean value of range for the pass. Plots are made for range rate o-c vs range for the time periods (a) May 24—June 24, 1967 and (b) July 1-15, 1967.

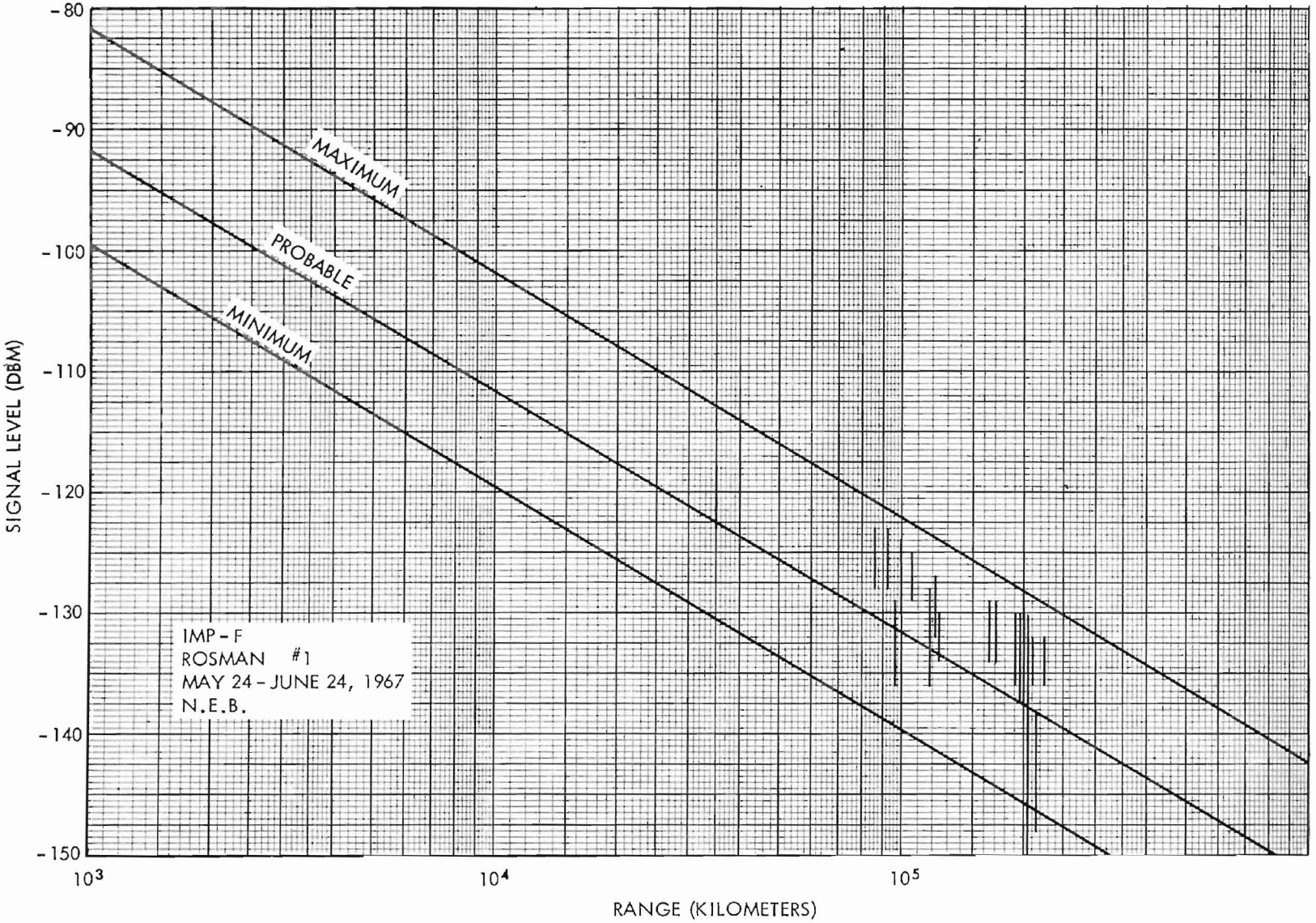
-80
-90
-100
-110
-120
-130
-140
-150
SIGNAL LEVEL (DBM)
MAXIMUM
PROBABLE
MINIMUM
IMP - F
ROSMAN #1
MAY 24 - JUNE 24, 1967
N.E.B.
10^3
10^4
10^5
RANGE (KILOMETERS)

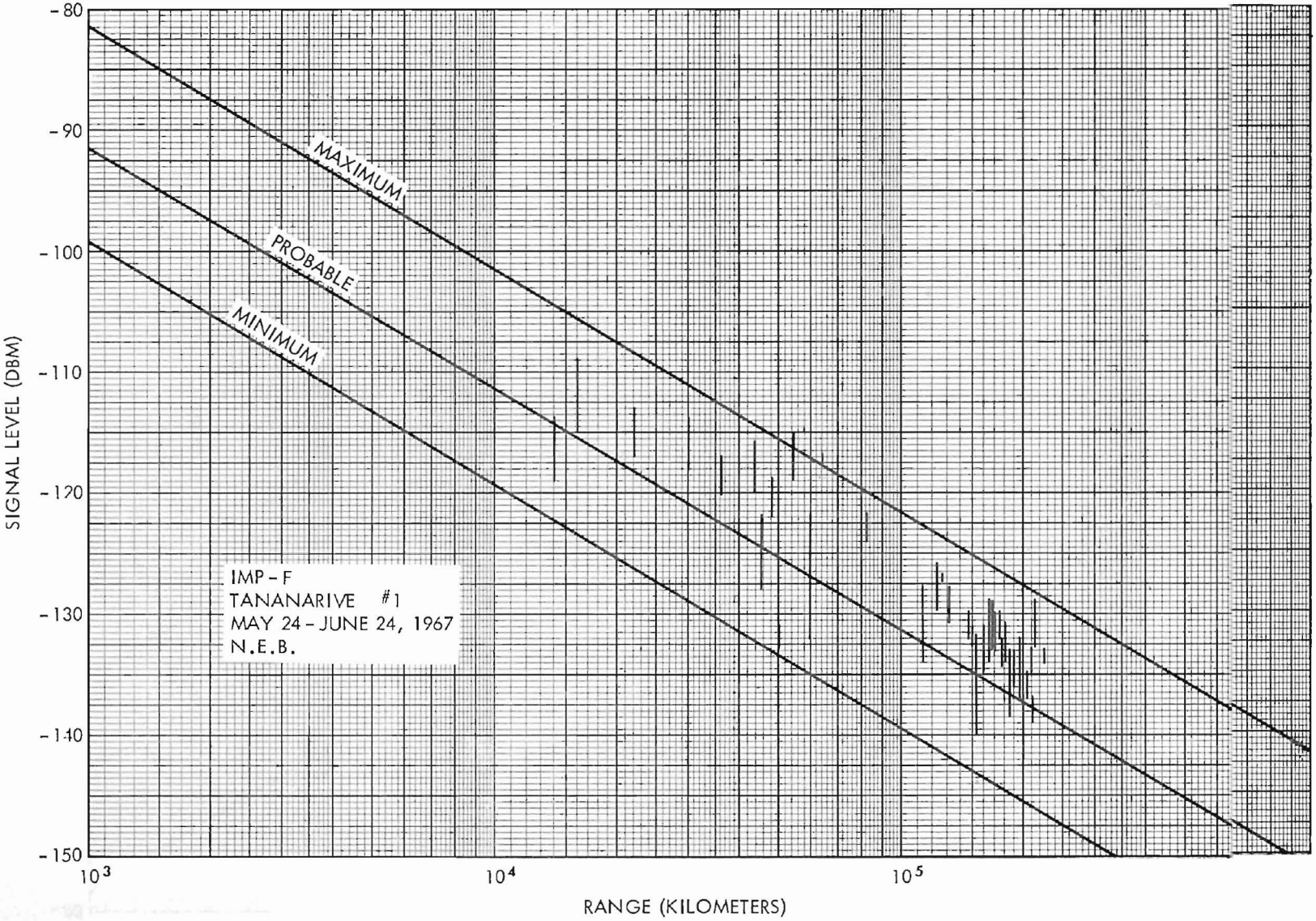
-80
-90
-100
-110
-120
-130
-140
-150
SIGNAL LEVEL (DBM)
MAXIMUM
PROBABLE
MINIMUM
IMP - F
TANANARIVE #1
MAY 24 - JUNE 24, 1967
N.E.B.
10^3
10^4
10^5
RANGE (KILOMETERS)

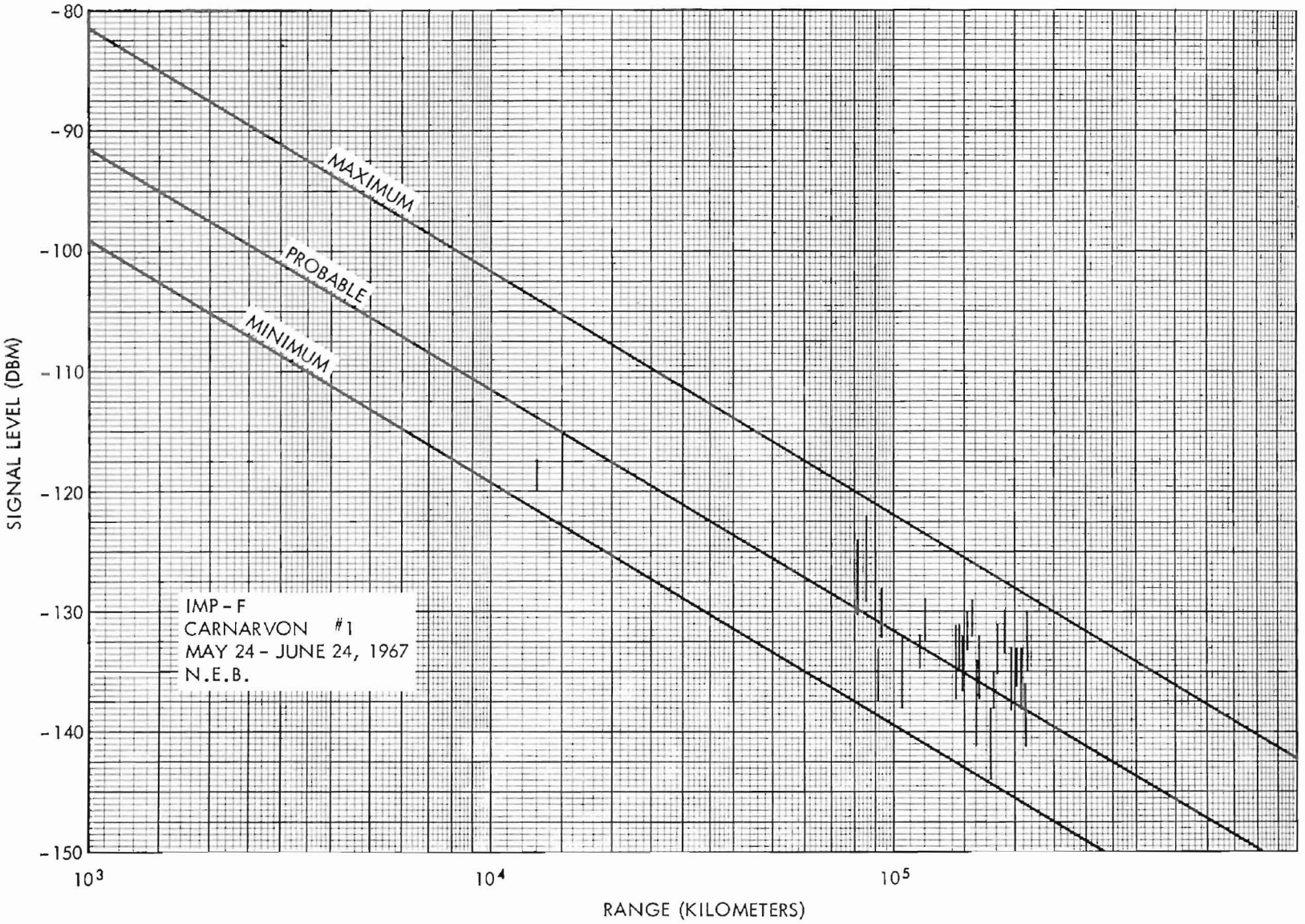
-80
-90
-100
-110
-120
-130
-140
-150
SIGNAL LEVEL (DBM)
MAXIMUM
PROBABLE
MINIMUM
IMP - F
CARNARVON #1
MAY 24 - JUNE 24, 1967
N.E.B.
10^3
10^4
10^5
RANGE (KILOMETERS)

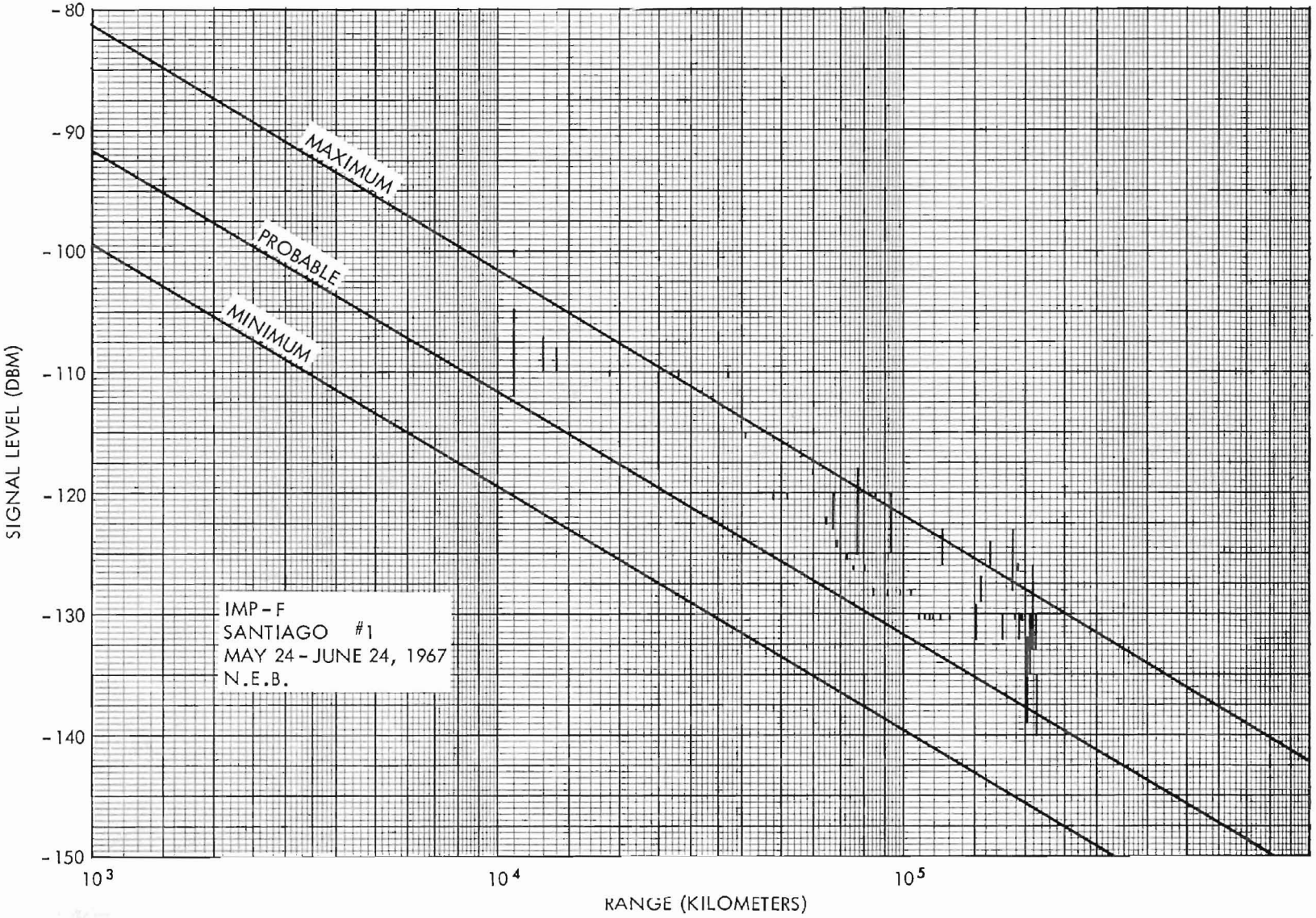
-80
-90
-100
-110
-120
-130
-140
-150
SIGNAL LEVEL (DBM)
MAXIMUM
PROBABLE
MINIMUM
IMP-F
SANTIAGO #1
MAY 24 - JUNE 24, 1967
N.E.B.
10^3
10^4
10^5
RANGE (KILOMETERS)

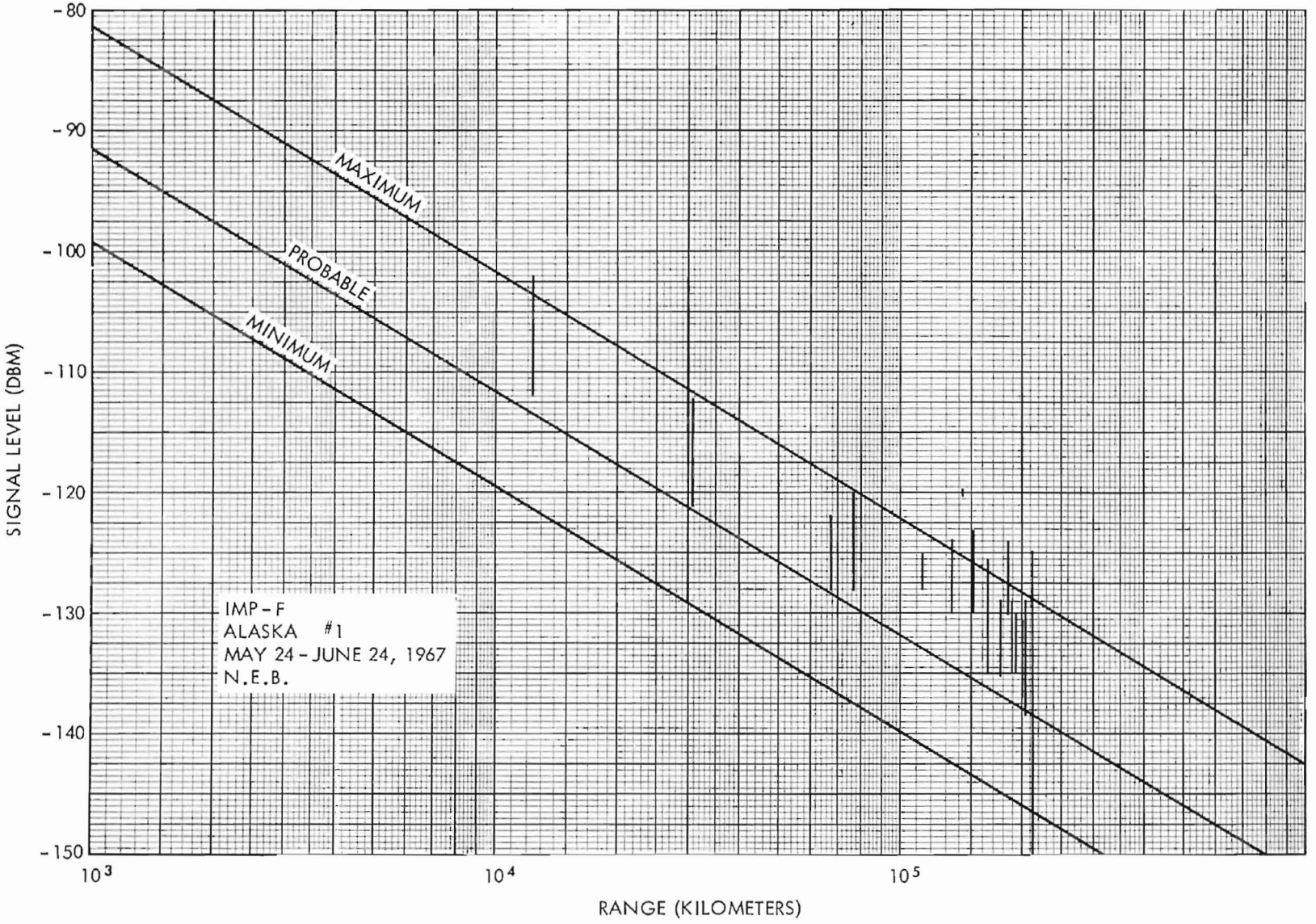
-80
-90
-100
-110
-120
-130
-140
-150
SIGNAL LEVEL (DBM)
MAXIMUM
PROBABLE
MINIMUM
IMP-F
ALASKA #1
MAY 24 - JUNE 24, 1967
N.E.B.
10^3
10^4
10^5
RANGE (KILOMETERS)

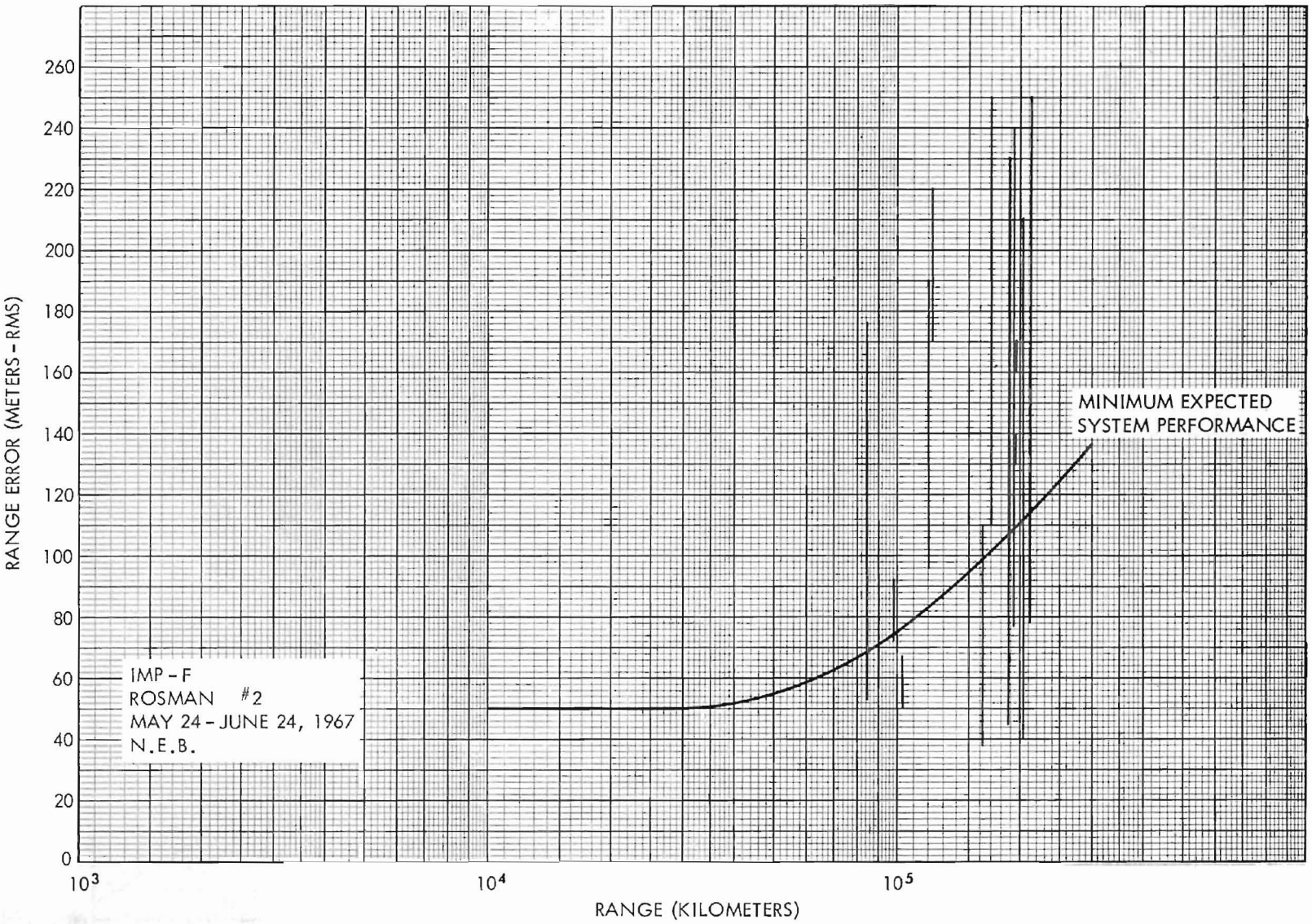
RANGE ERROR (METERS - RMS)
260
240
220
200
180
160
140
120
100
80
60
40
20
0
10^3
10^4
10^5
RANGE (KILOMETERS)
MINIMUM EXPECTED
SYSTEM PERFORMANCE
IMP - F
ROSMAN #2
MAY 24 - JUNE 24, 1967
N.E.B.

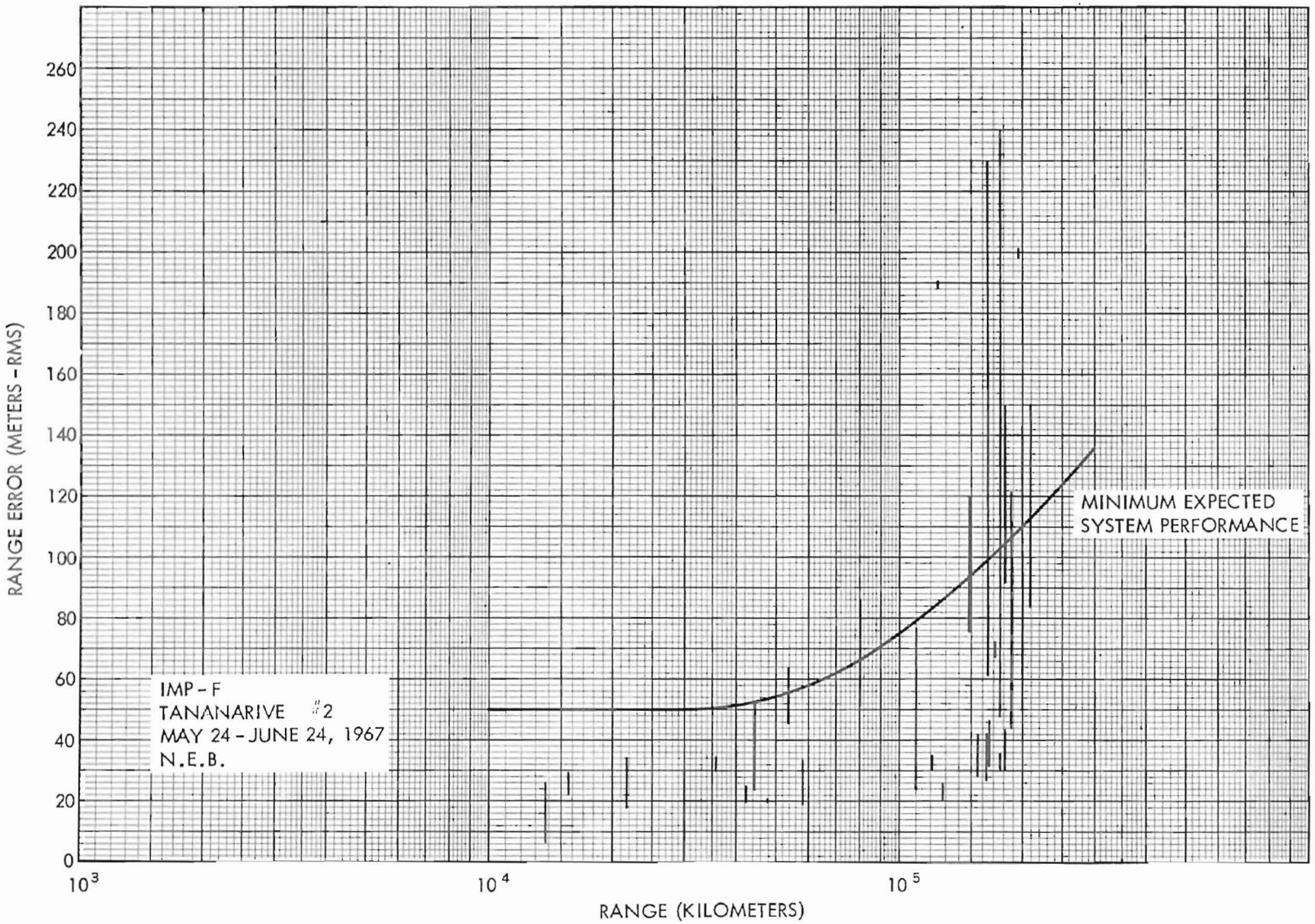
RANGE ERROR (METERS - RMS)
260
240
220
200
180
160
140
120
100
80
60
40
20
0
10^3
10^4
10^5
RANGE (KILOMETERS)
IMP - F
TANANARIVE #2
MAY 24 - JUNE 24, 1967
N.E.B.
MINIMUM EXPECTED
SYSTEM PERFORMANCE

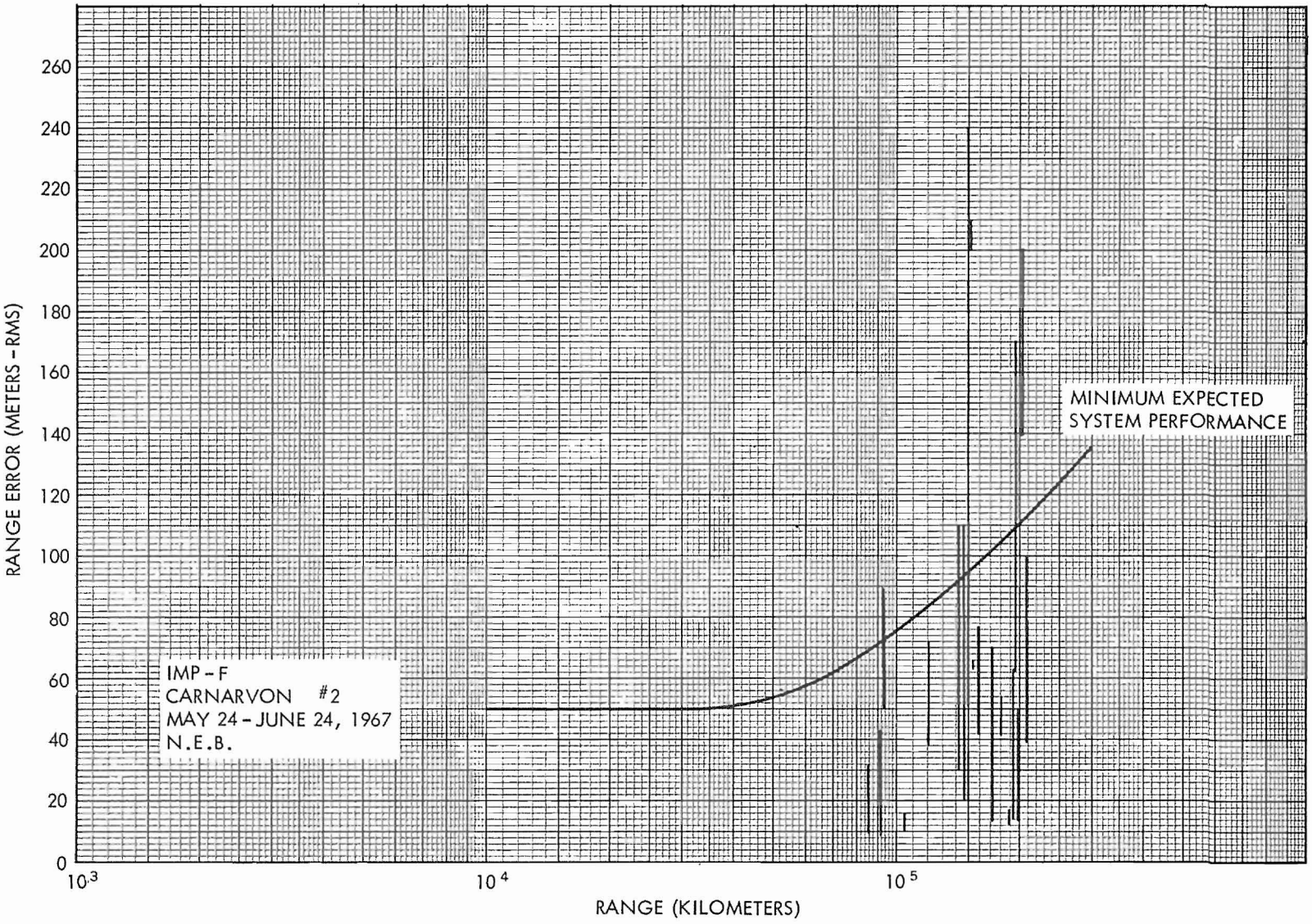
RANGE ERROR (METERS - RMS)
260
240
220
200
180
160
140
120
100
80
60
40
20
0
10^3
10^4
10^5
RANGE (KILOMETERS)
MINIMUM EXPECTED
SYSTEM PERFORMANCE
IMP - F
CARNARVON #2
MAY 24 - JUNE 24, 1967
N.E.B.

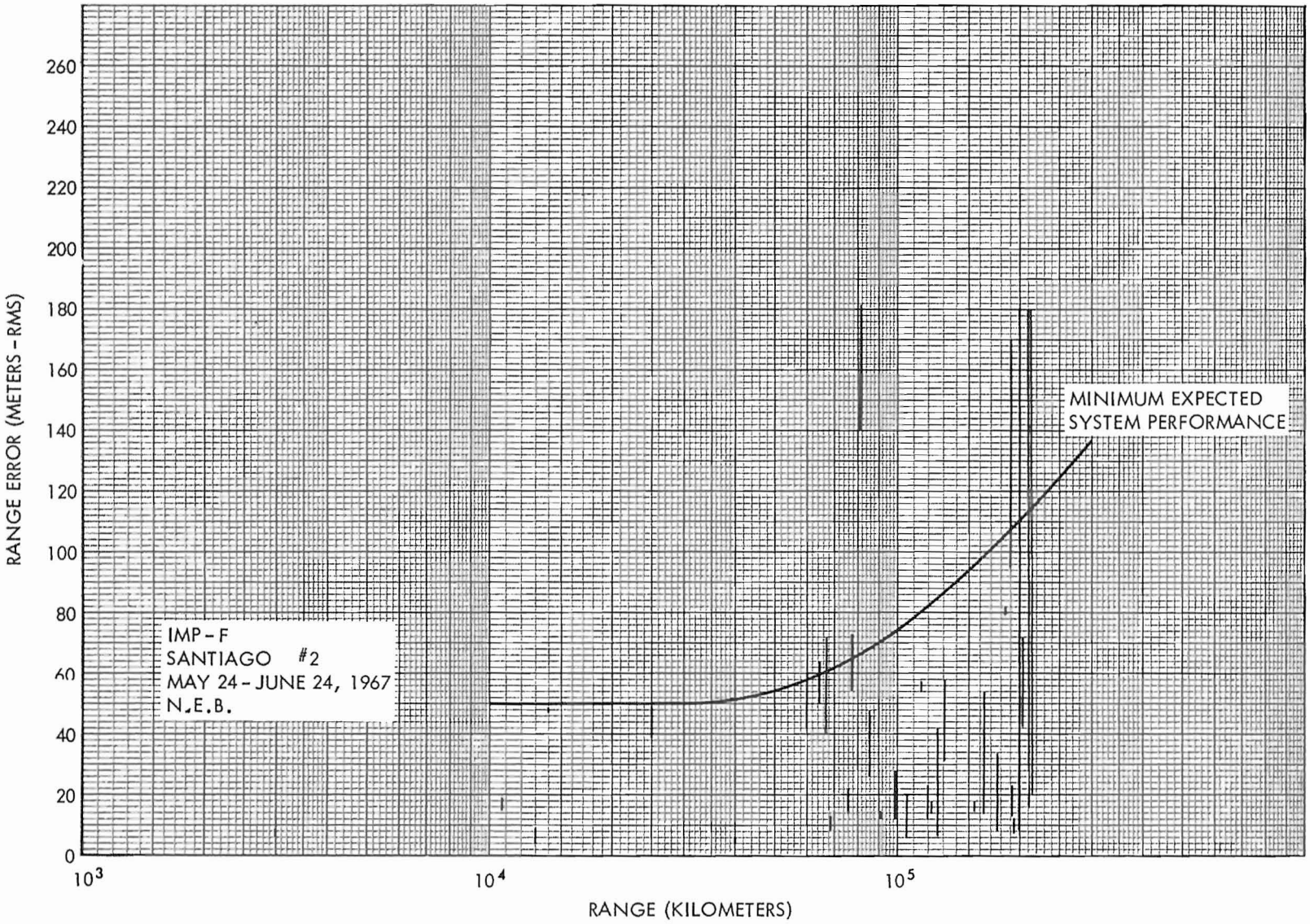
RANGE ERROR (METERS - RMS)
260
240
220
200
180
160
140
120
100
80
60
40
20
0
10^3
10^4
10^5
RANGE (KILOMETERS)
MINIMUM EXPECTED
SYSTEM PERFORMANCE
IMP - F
SANTIAGO #2
MAY 24 - JUNE 24, 1967
N.E.B.

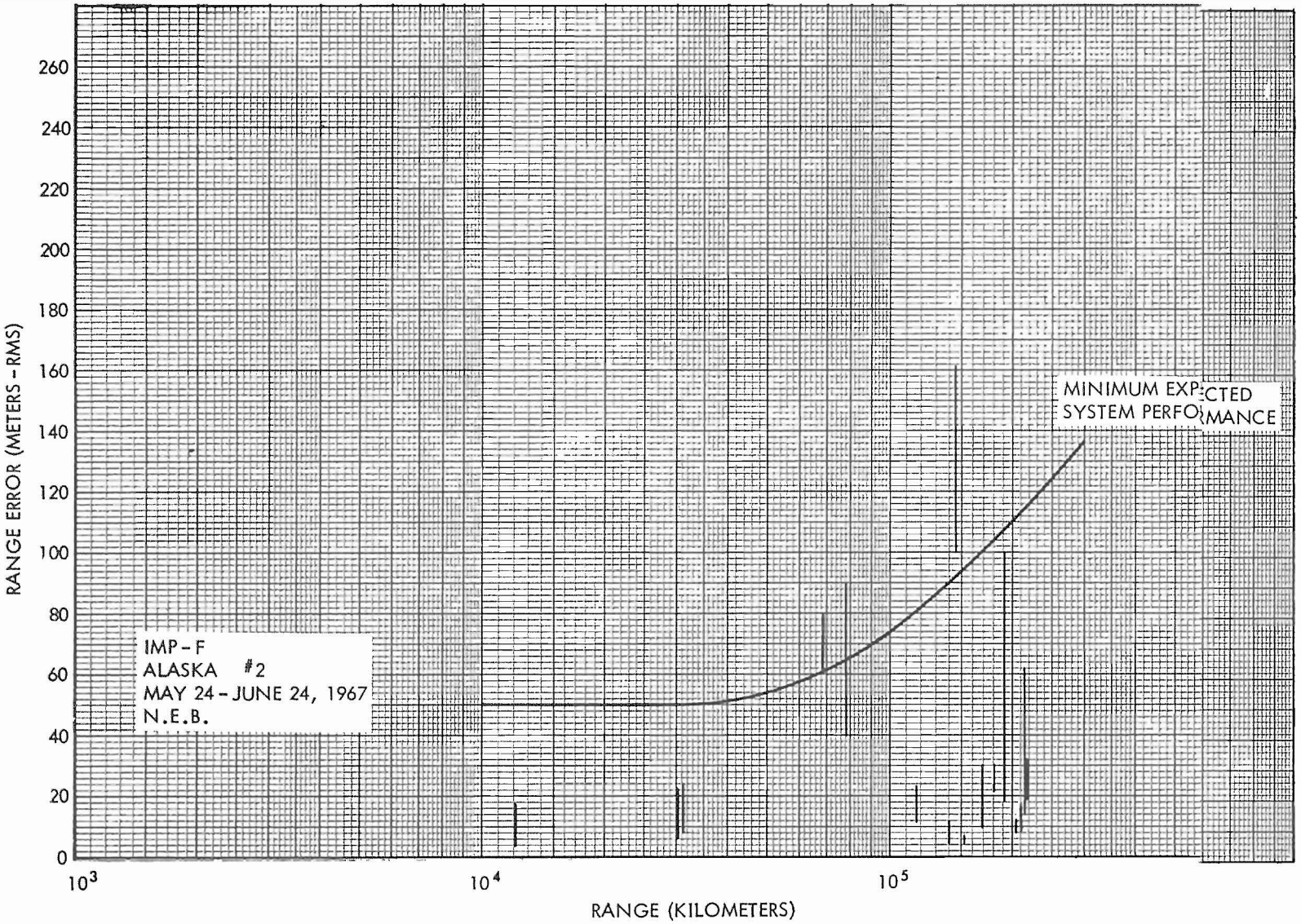
RANGE ERROR (METERS - RMS)
260
240
220
200
180
160
140
120
100
80
60
40
20
0
10^3
10^4
10^5
RANGE (KILOMETERS)
IMP - F
ALASKA #2
MAY 24 - JUNE 24, 1967
N.E.B.
MINIMUM EXPECTED
SYSTEM PERFORMANCE

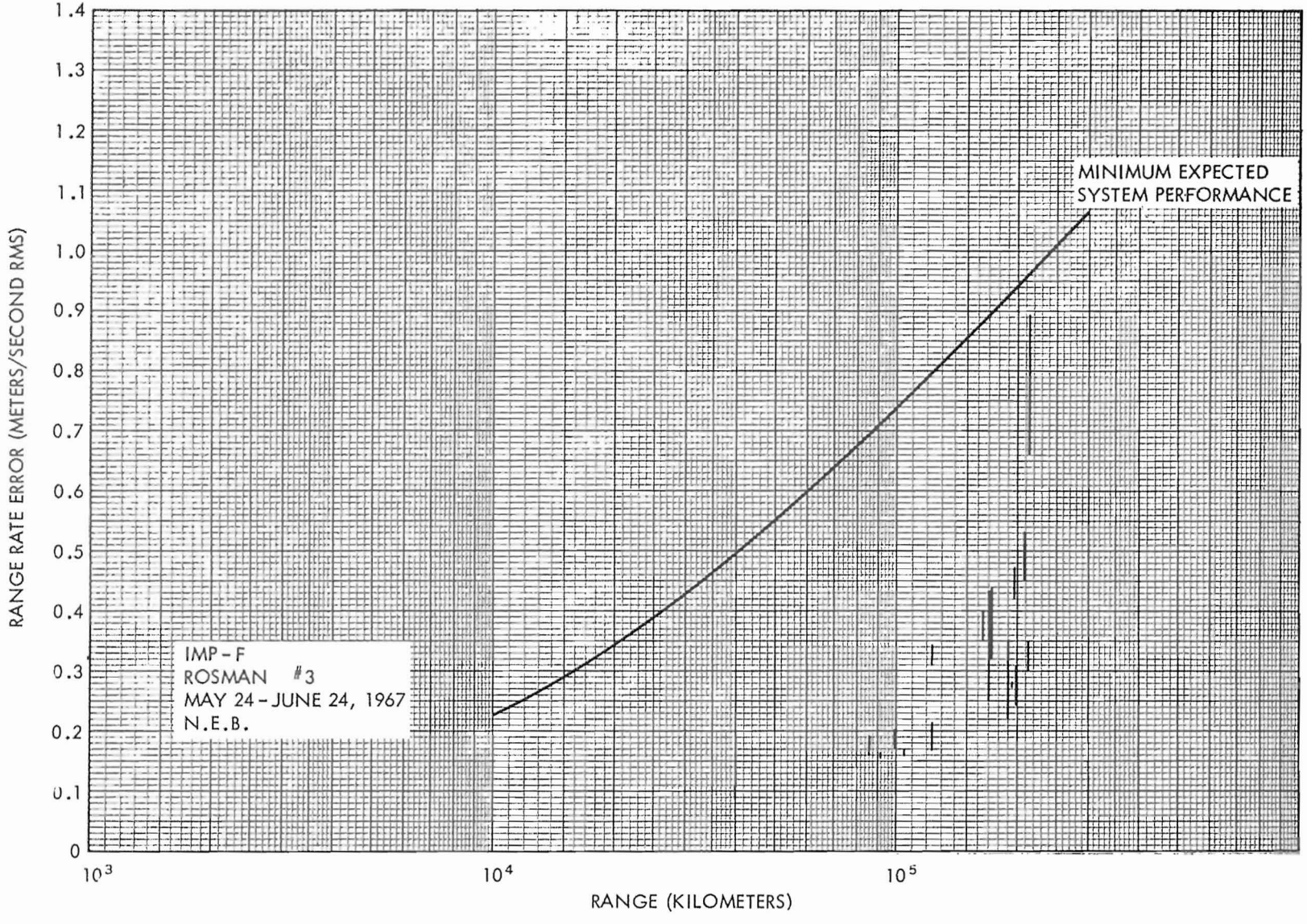
RANGE RATE ERROR (METERS/SECOND RMS)
1.4
1.3
1.2
1.1
1.0
0.9
0.8
0.7
0.6
0.5
0.4
0.3
0.2
0.1
0
10^3
10^4
10^5
RANGE (KILOMETERS)
MINIMUM EXPECTED
SYSTEM PERFORMANCE
IMP - F
ROSMAN #3
MAY 24 - JUNE 24, 1967
N.E.B.

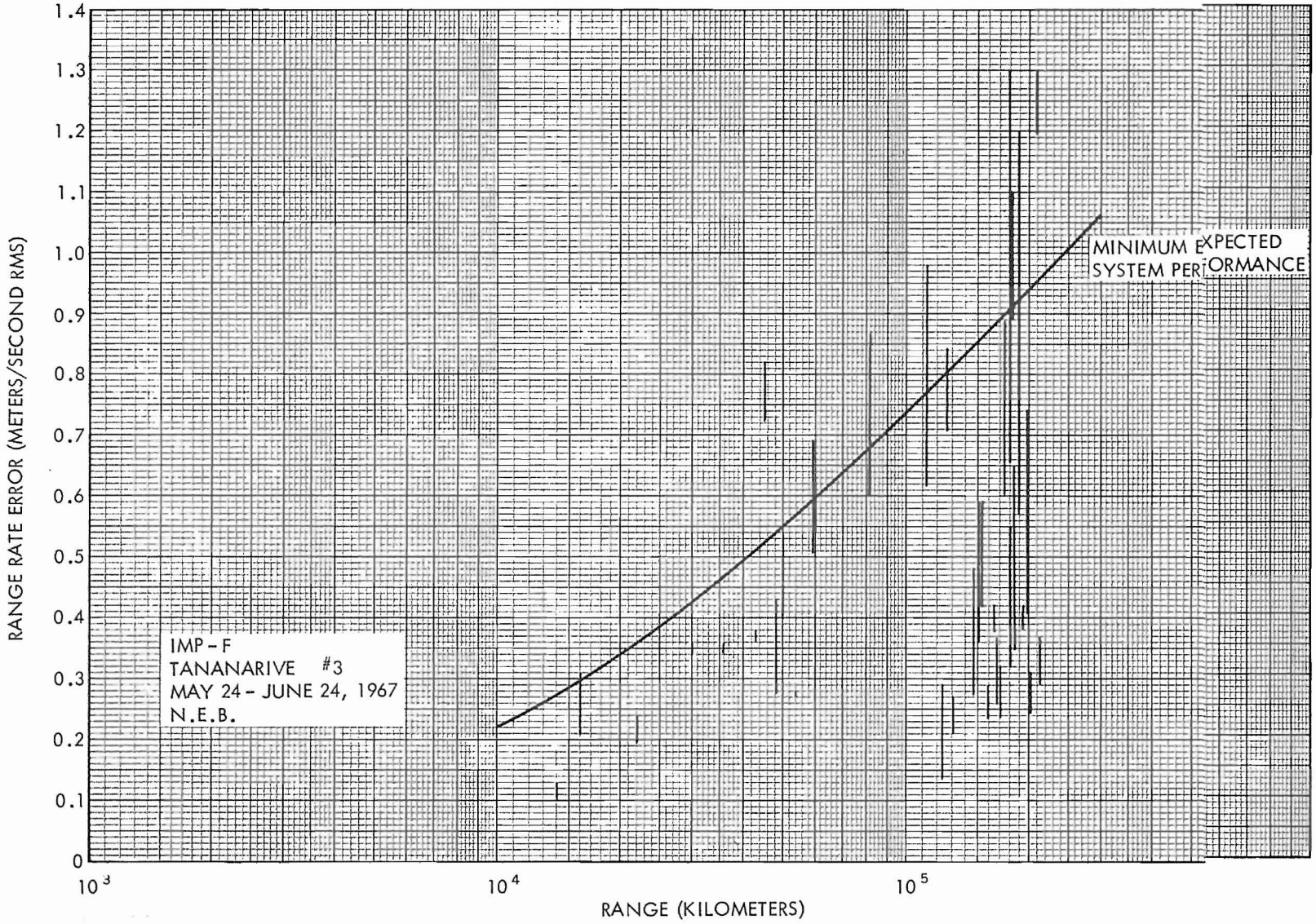
RANGE RATE ERROR (METERS/SECOND RMS)
1.4
1.3
1.2
1.1
1.0
0.9
0.8
0.7
0.6
0.5
0.4
0.3
0.2
0.1
0
10^3
10^4
10^5
RANGE (KILOMETERS)
MINIMUM EXPECTED SYSTEM PERFORMANCE
IMP - F
TANANARIVE #3
MAY 24 - JUNE 24, 1967
N.E.B.

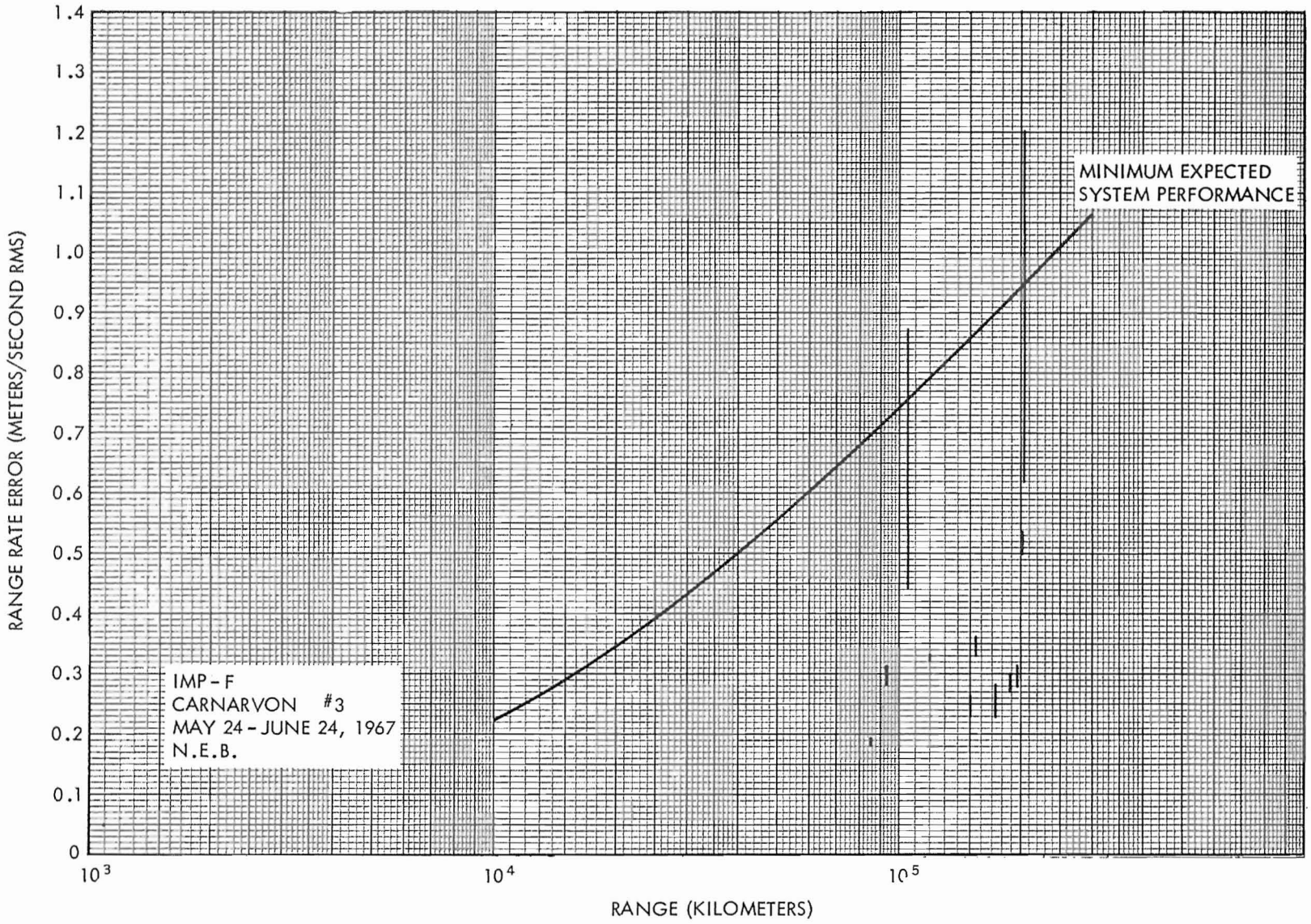
RANGE RATE ERROR (METERS/SECOND RMS)
1.4
1.3
1.2
1.1
1.0
0.9
0.8
0.7
0.6
0.5
0.4
0.3
0.2
0.1
0
10^3
10^4
10^5
RANGE (KILOMETERS)
MINIMUM EXPECTED
SYSTEM PERFORMANCE
IMP-F
CARNARVON #3
MAY 24 - JUNE 24, 1967
N.E.B.

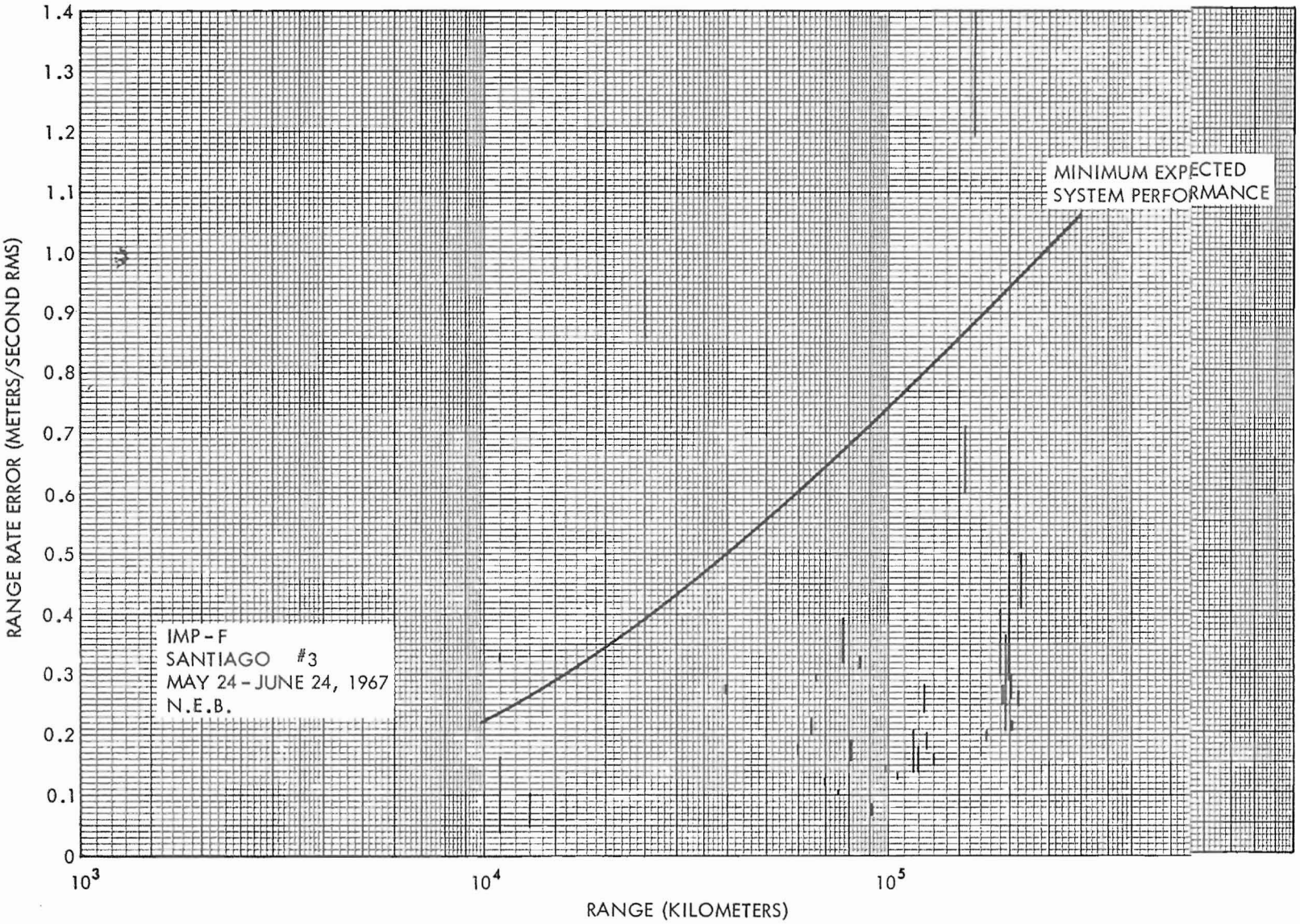
RANGE RATE ERROR (METERS/SECOND RMS)
1.4
1.3
1.2
1.1
1.0
0.9
0.8
0.7
0.6
0.5
0.4
0.3
0.2
0.1
0
10^3
10^4
10^5
RANGE (KILOMETERS)
MINIMUM EXPECTED SYSTEM PERFORMANCE
IMP-F
SANTIAGO #3
MAY 24 - JUNE 24, 1967
N.E.B.

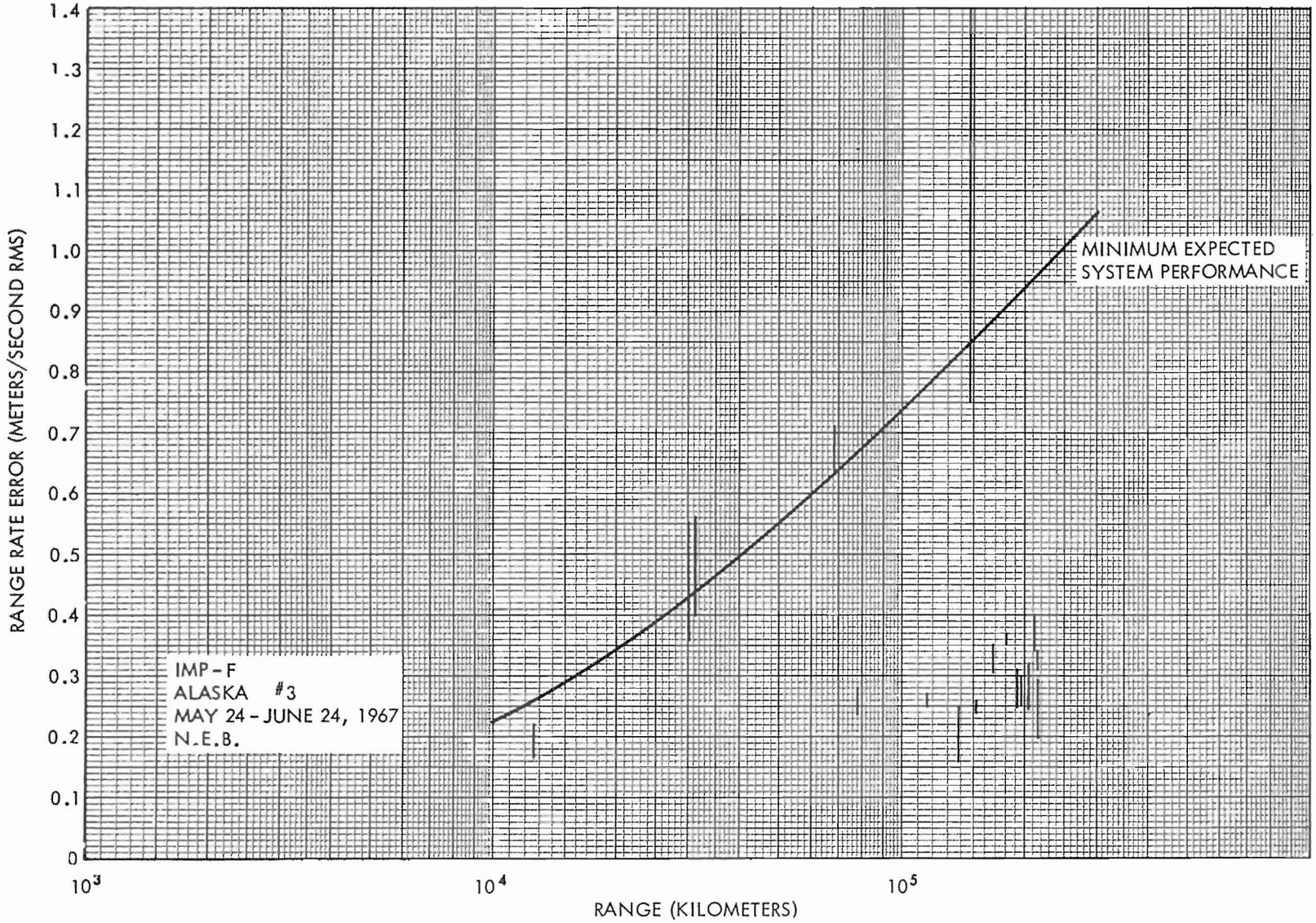
RANGE RATE ERROR (METERS/SECOND RMS)
1.4
1.3
1.2
1.1
1.0
0.9
0.8
0.7
0.6
0.5
0.4
0.3
0.2
0.1
0
10^3
10^4
10^5
RANGE (KILOMETERS)
MINIMUM EXPECTED
SYSTEM PERFORMANCE
IMP-F
ALASKA #3
MAY 24 - JUNE 24, 1967
N.E.B.

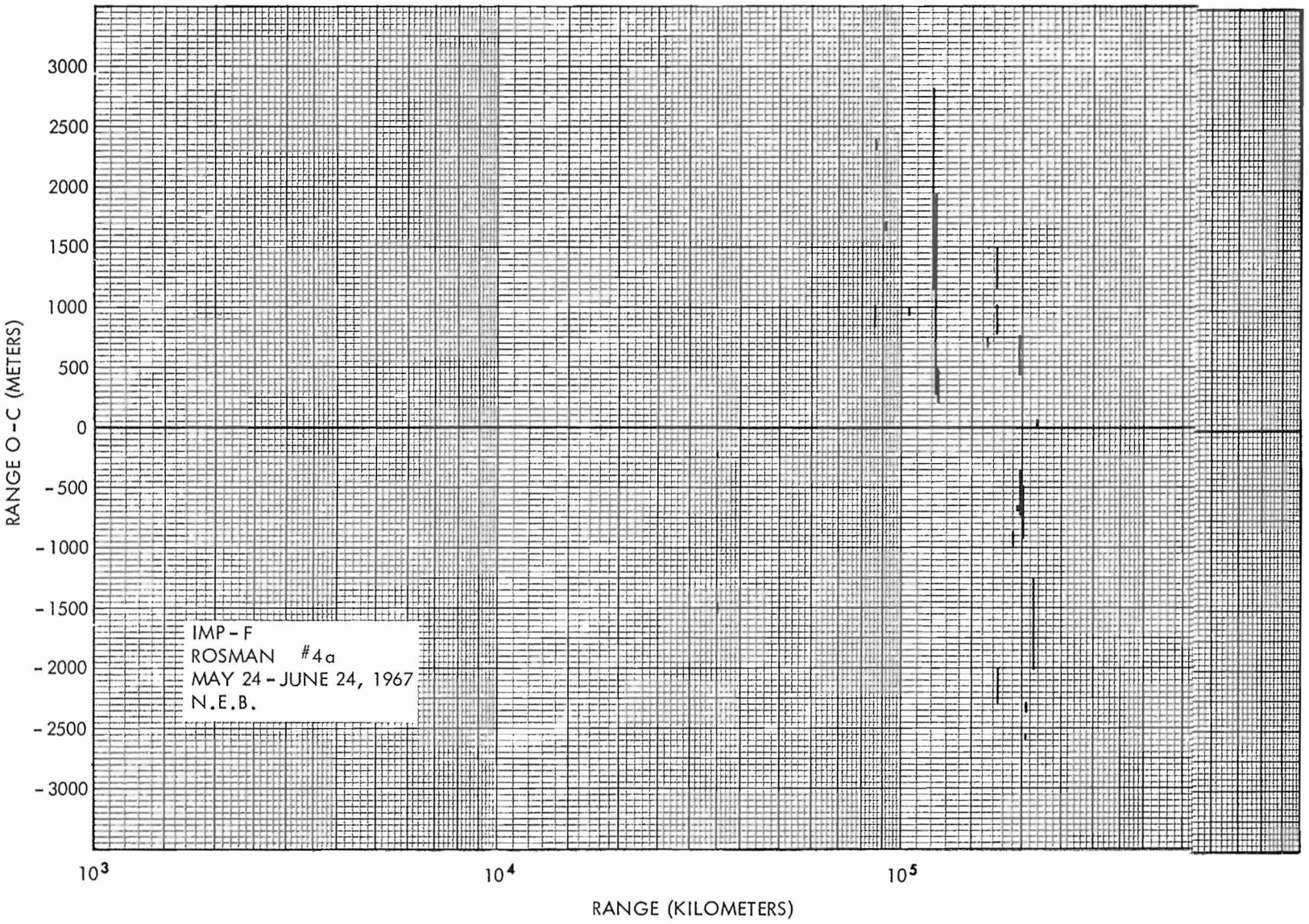
3000
2500
2000
1500
1000
500
0
- 500
- 1000
- 1500
- 2000
- 2500
- 3000
RANGE O-C (METERS)
IMP-F
ROSMAN #4a
MAY 24 - JUNE 24, 1967
N.E.B.
10^3
10^4
10^5
RANGE (KILOMETERS)

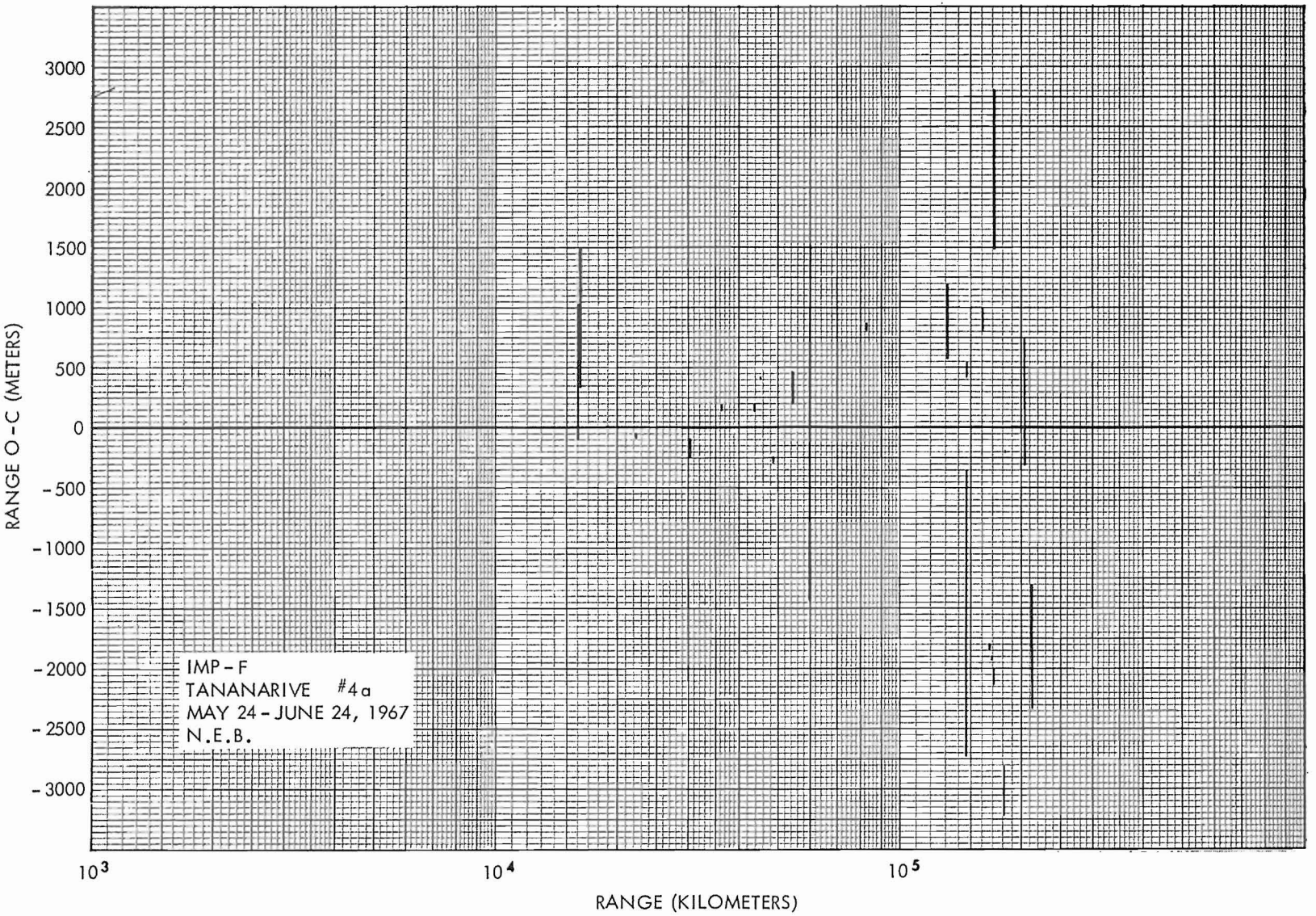
3000
2500
2000
1500
1000
500
0
-500
-1000
-1500
-2000
-2500
-3000
RANGE O-C (METERS)
IMP-F
TANANARIVE #4a
MAY 24-JUNE 24, 1967
N.E.B.
10^3
10^4
10^5
RANGE (KILOMETERS)

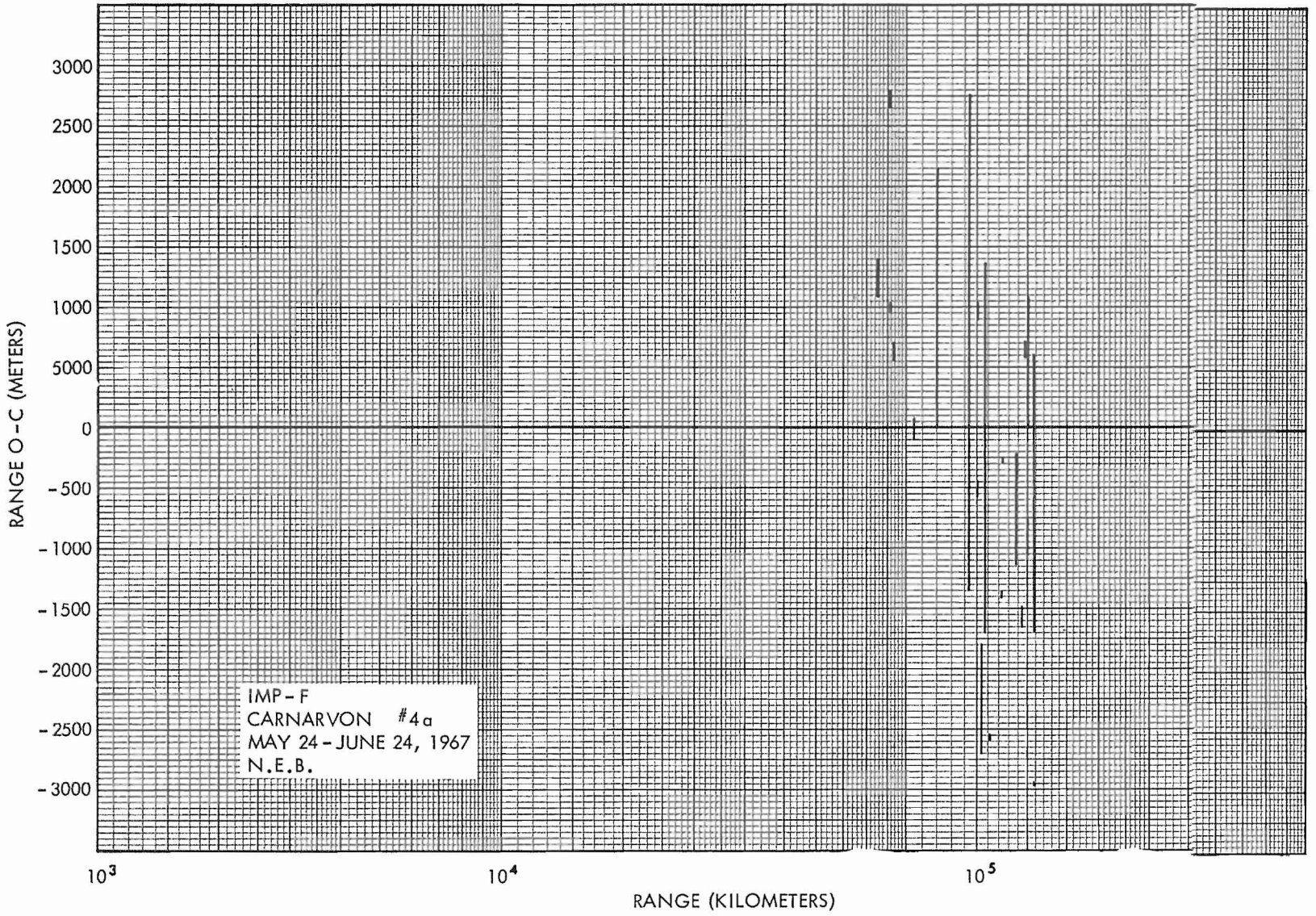
3000
2500
2000
1500
1000
500
0
-500
-1000
-1500
-2000
-2500
-3000
RANGE O-C (METERS)
IMP-F
CARNARVON #4a
MAY 24-JUNE 24, 1967
N.E.B.
10^3
10^4
10^5
RANGE (KILOMETERS)

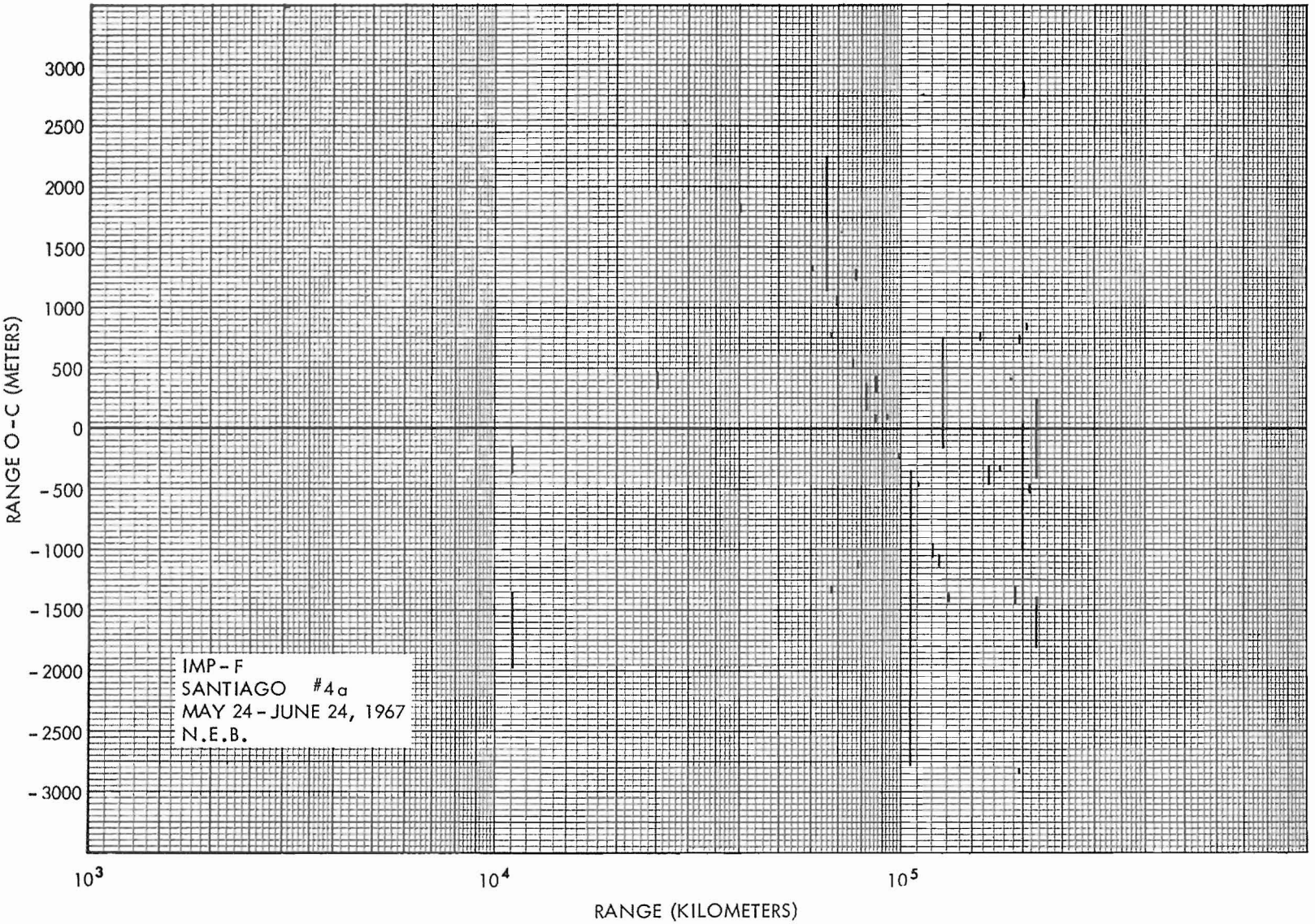
3000
2500
2000
1500
1000
500
0
-500
-1000
-1500
-2000
-2500
-3000
RANGE O-C (METERS)
IMP-F
SANTIAGO #4a
MAY 24 - JUNE 24, 1967
N.E.B.
10^3
10^4
10^5
RANGE (KILOMETERS)

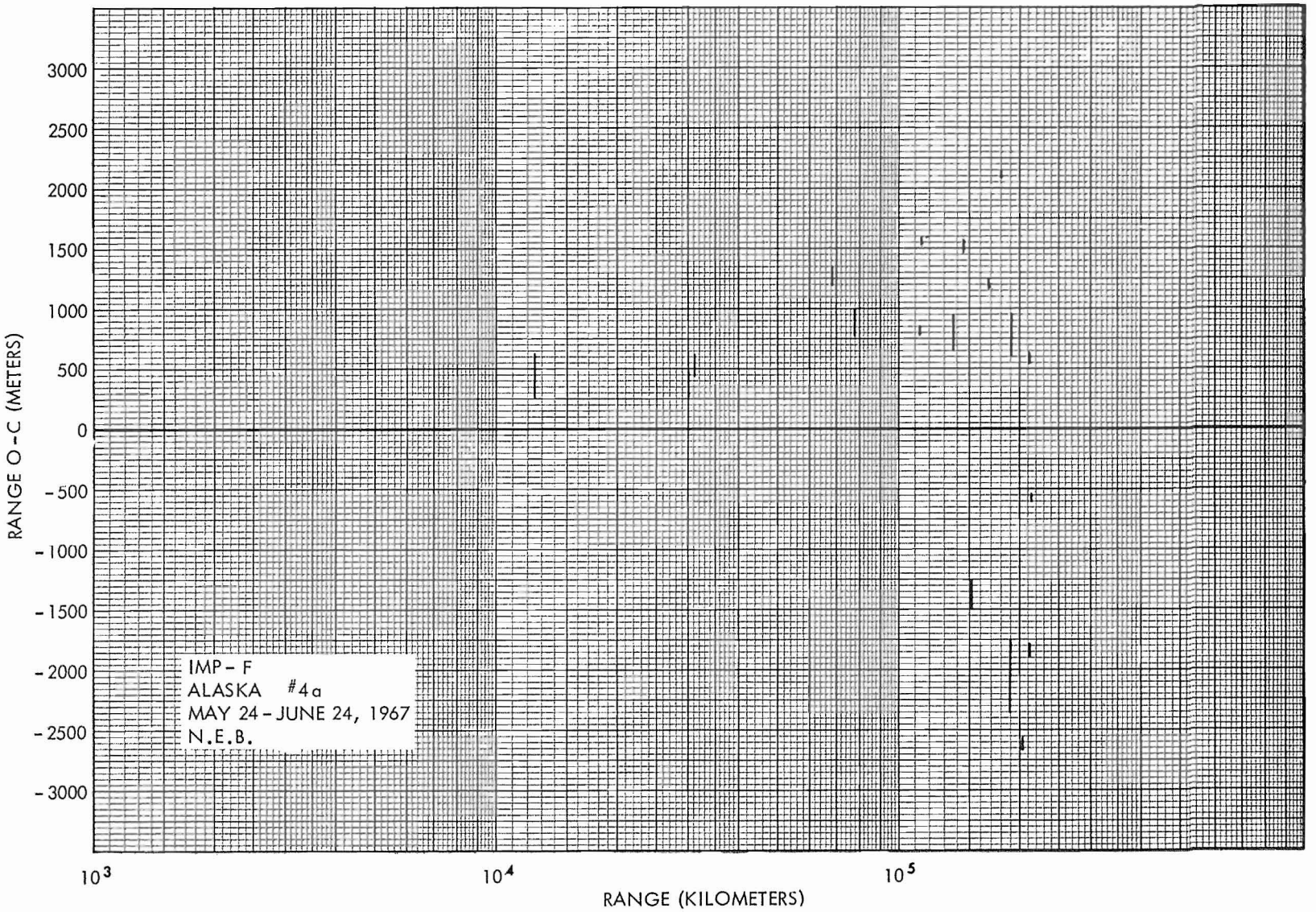
3000
2500
2000
1500
1000
500
0
-500
-1000
-1500
-2000
-2500
-3000
RANGE O-C (METERS)
IMP-F
ALASKA #4a
MAY 24-JUNE 24, 1967
N.E.B.
10^3
10^4
10^5
RANGE (KILOMETERS)

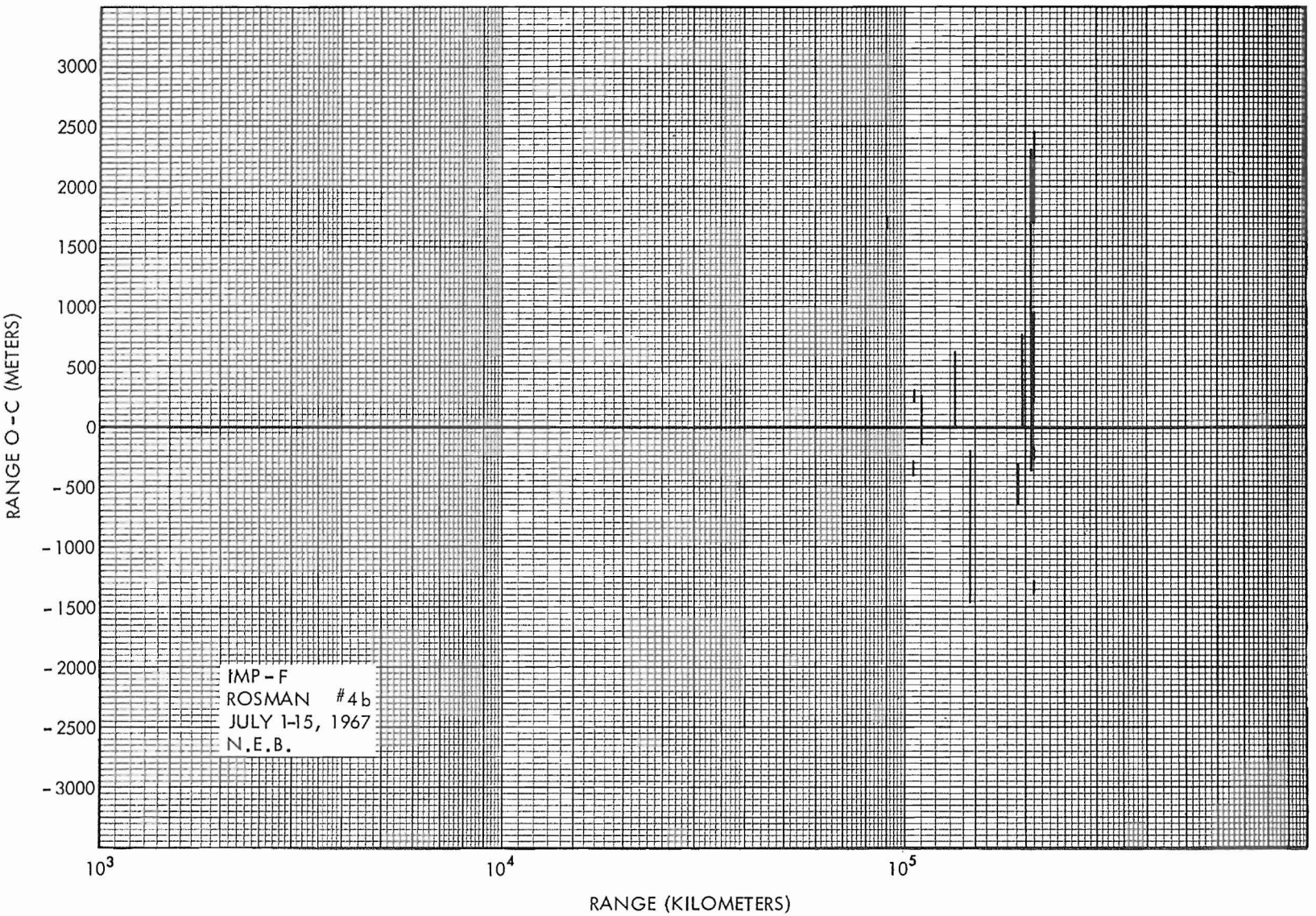
3000
2500
2000
1500
1000
500
0
- 500
- 1000
- 1500
- 2000
- 2500
- 3000
RANGE O-C (METERS)
IMP-F
ROSMAN #4b
JULY 1-15, 1967
N.E.B.
10^3
10^4
10^5
RANGE (KILOMETERS)

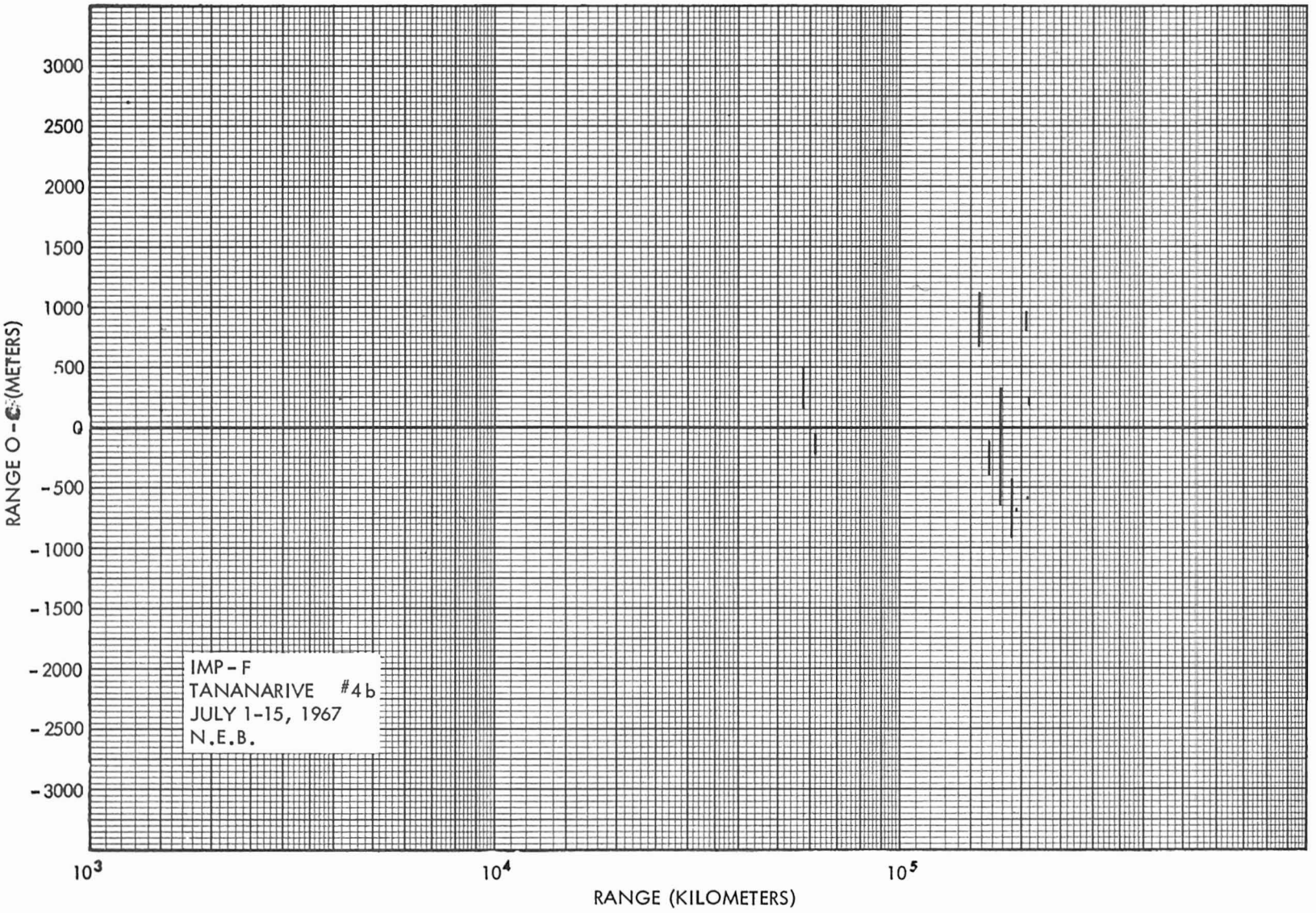
3000
2500
2000
1500
1000
500
0
-500
-1000
-1500
-2000
-2500
-3000
RANGE O-C (METERS)
IMP-F
TANANARIVE #4b
JULY 1-15, 1967
N.E.B.
10^3
10^4
10^5
RANGE (KILOMETERS)

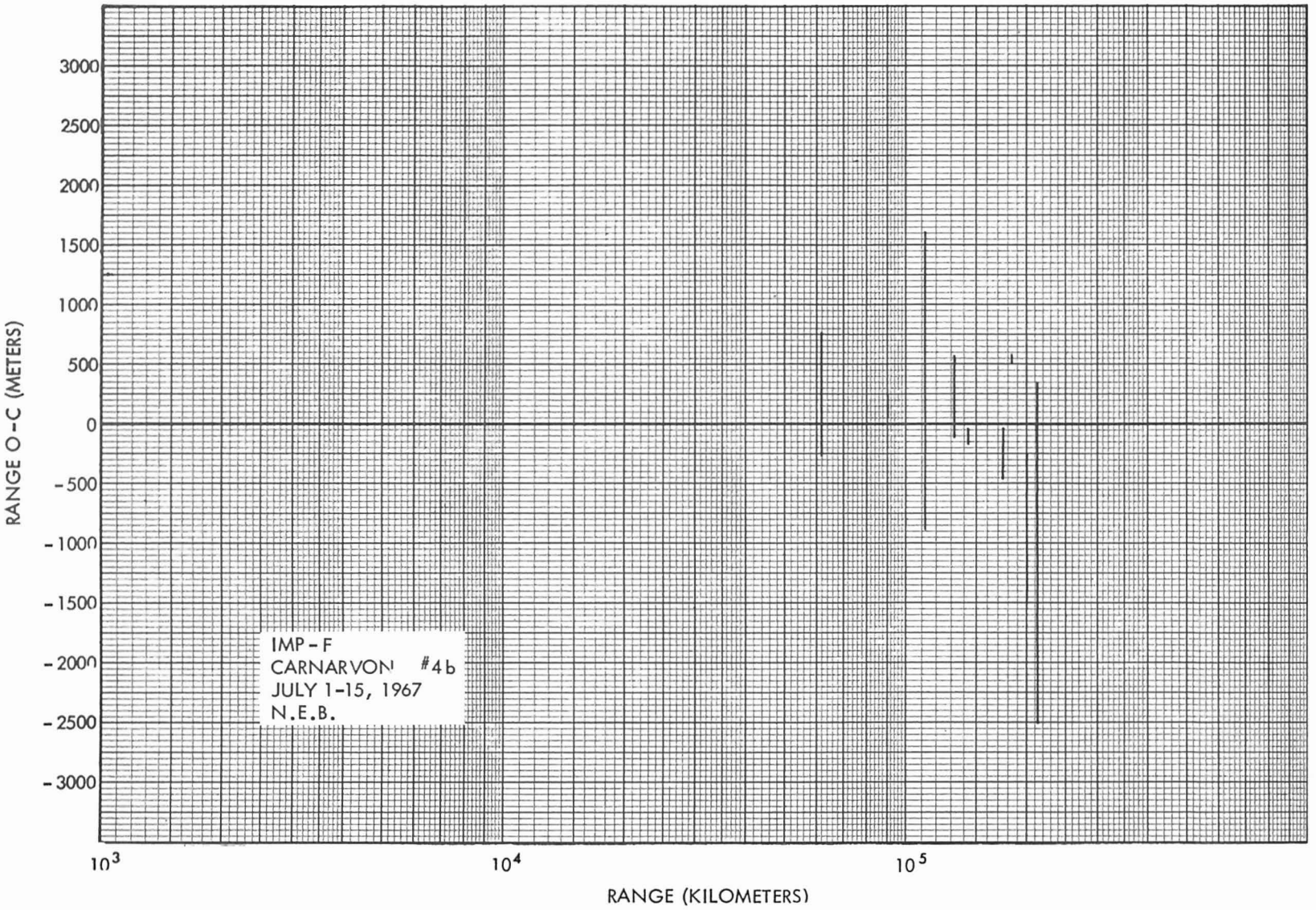
3000
2500
2000
1500
1000
500
0
-500
-1000
-1500
-2000
-2500
-3000
RANGE O-C (METERS)
IMP-F
CARNARVON #4b
JULY 1-15, 1967
N.E.B.
10^3
10^4
10^5
RANGE (KILOMETERS)

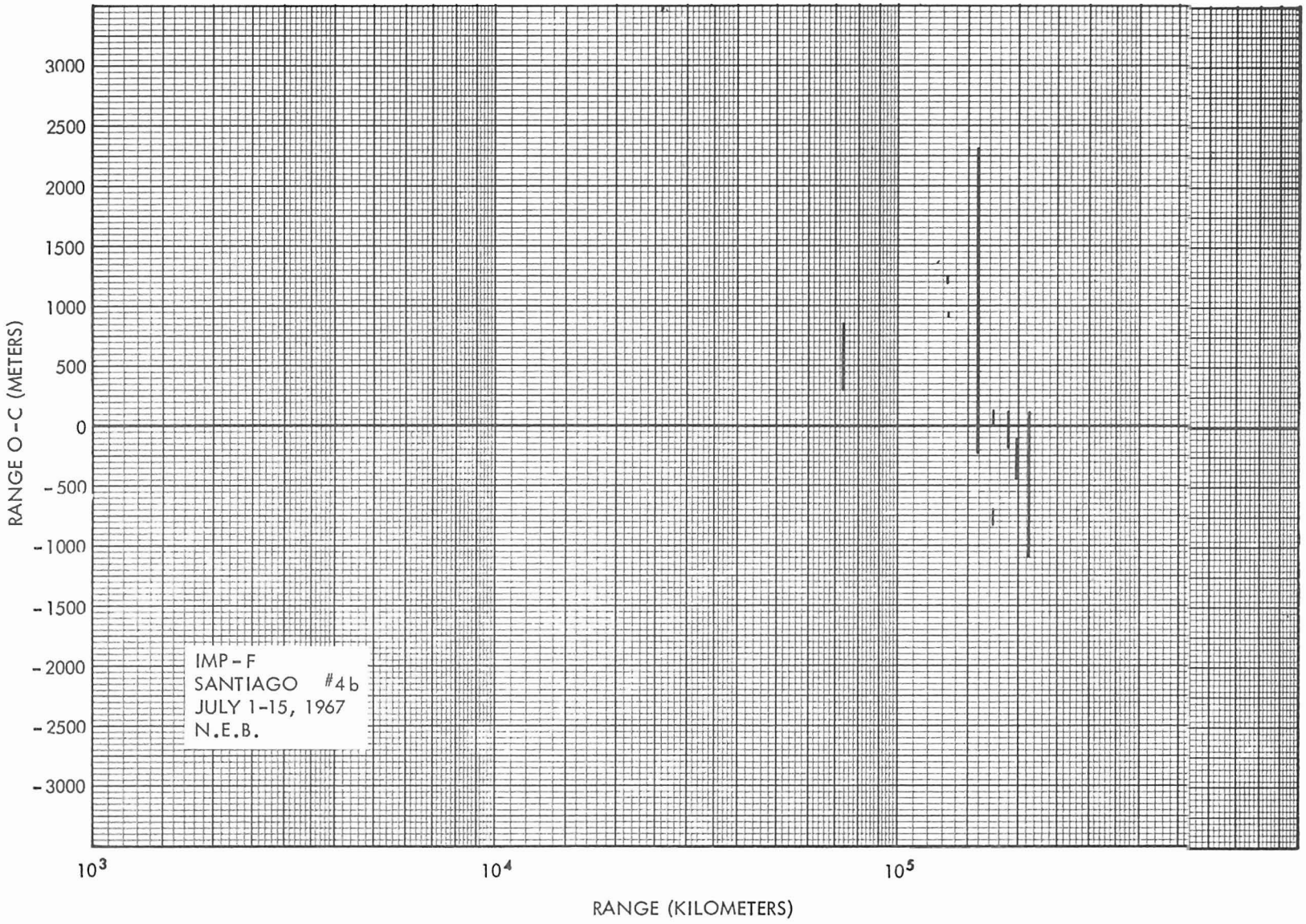
3000
2500
2000
1500
1000
500
0
-500
-1000
-1500
-2000
-2500
-3000
RANGE O-C (METERS)
IMP-F
SANTIAGO #4b
JULY 1-15, 1967
N.E.B.
10^3
10^4
10^5
RANGE (KILOMETERS)

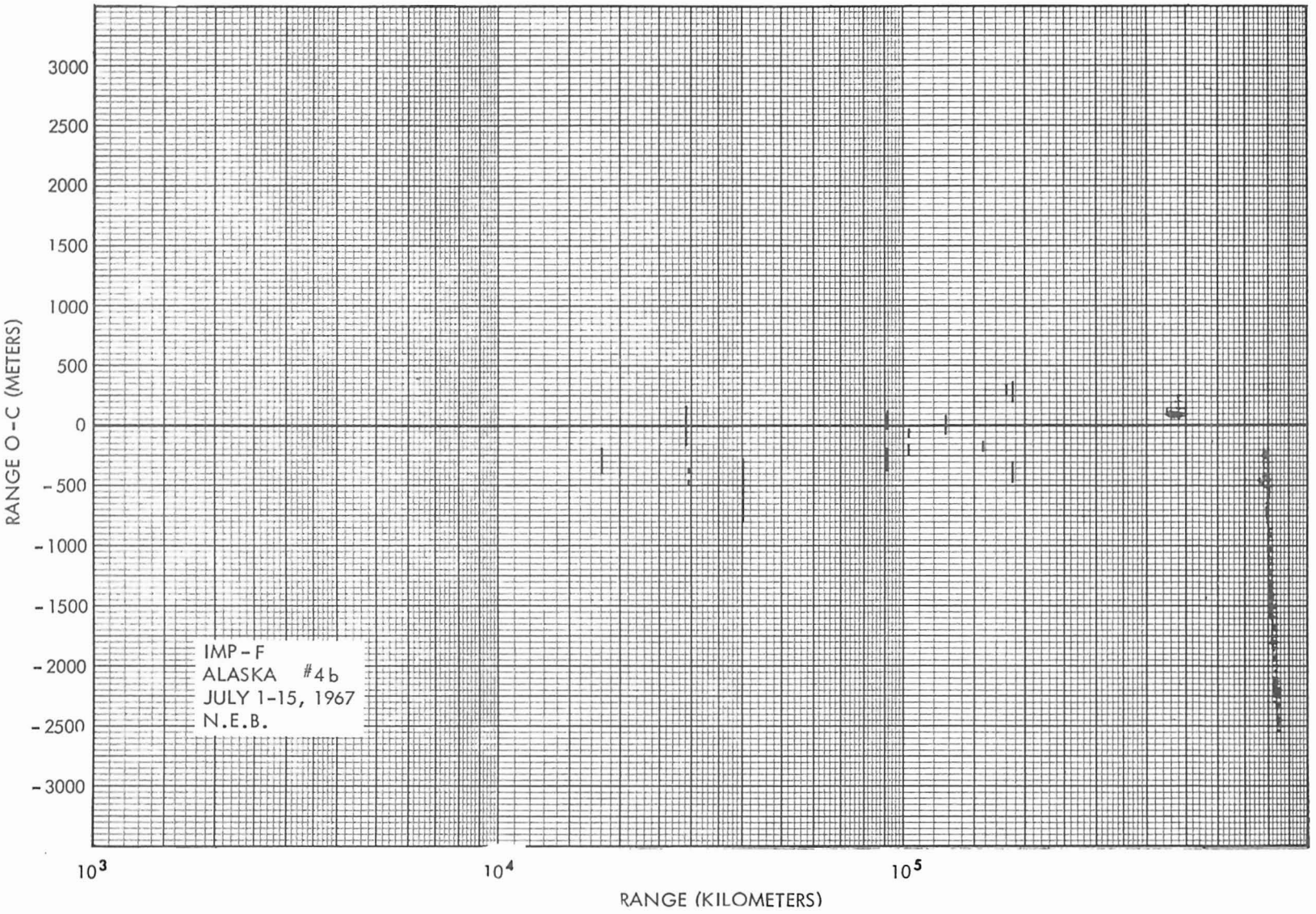
RANGE O-C (METERS)
3000
2500
2000
1500
1000
500
0
-500
-1000
-1500
-2000
-2500
-3000
IMP-F
ALASKA #4b
JULY 1-15, 1967
N.E.B.
10^3
10^4
10^5
RANGE (KILOMETERS)

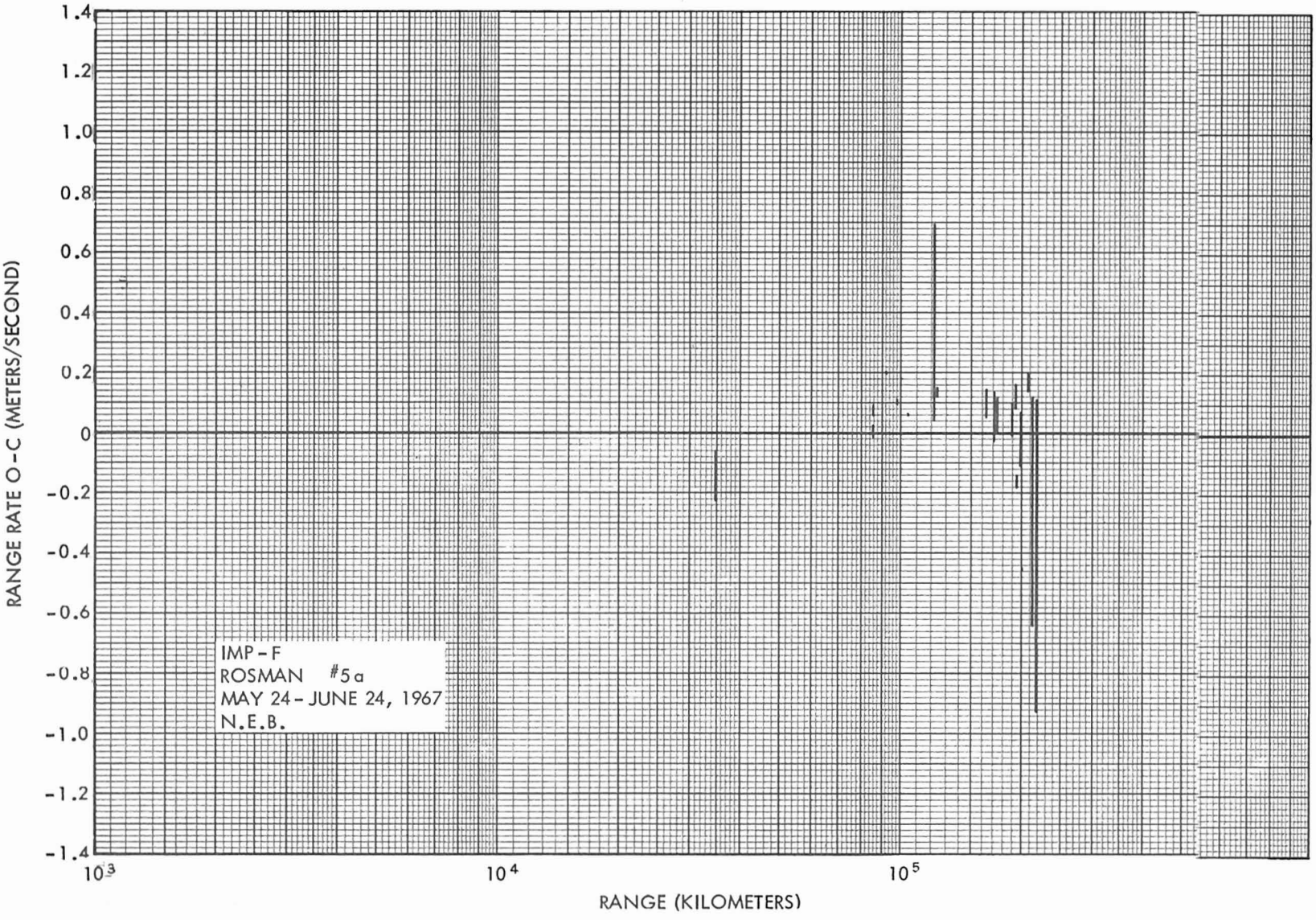
1.4
1.2
1.0
0.8
0.6
0.4
0.2
0
-0.2
-0.4
-0.6
-0.8
-1.0
-1.2
-1.4
RANGE RATE O-C (METERS/SECOND)
IMP-F
ROSMAN #5a
MAY 24 - JUNE 24, 1967
N.E.B.
10^3
10^4
10^5
RANGE (KILOMETERS)

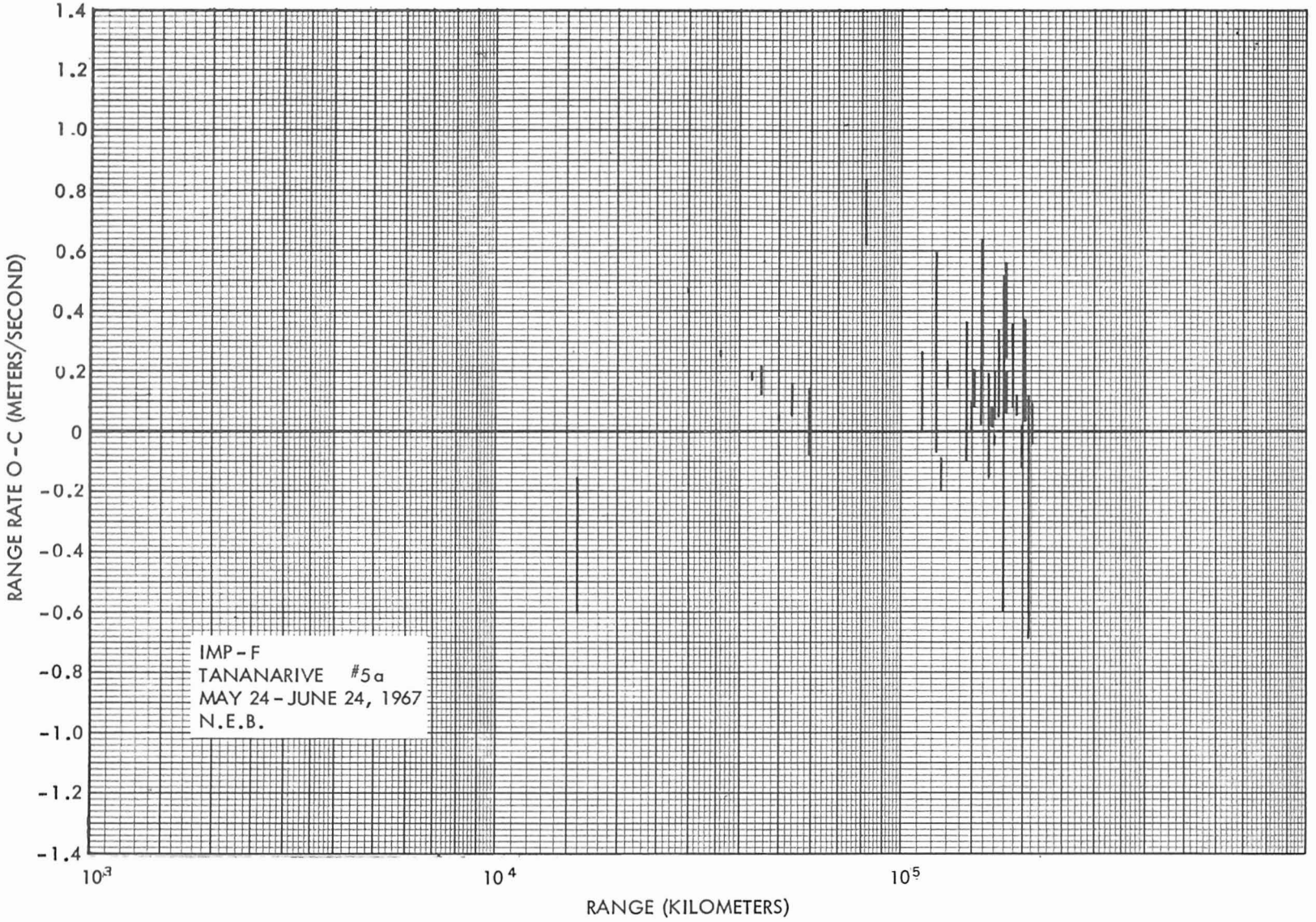
1.4
1.2
1.0
0.8
0.6
0.4
0.2
0
-0.2
-0.4
-0.6
-0.8
-1.0
-1.2
-1.4
RANGE RATE O-C (METERS/SECOND)
IMP-F
TANANARIVE #5a
MAY 24-JUNE 24, 1967
N.E.B.
10^3
10^4
10^5
RANGE (KILOMETERS)

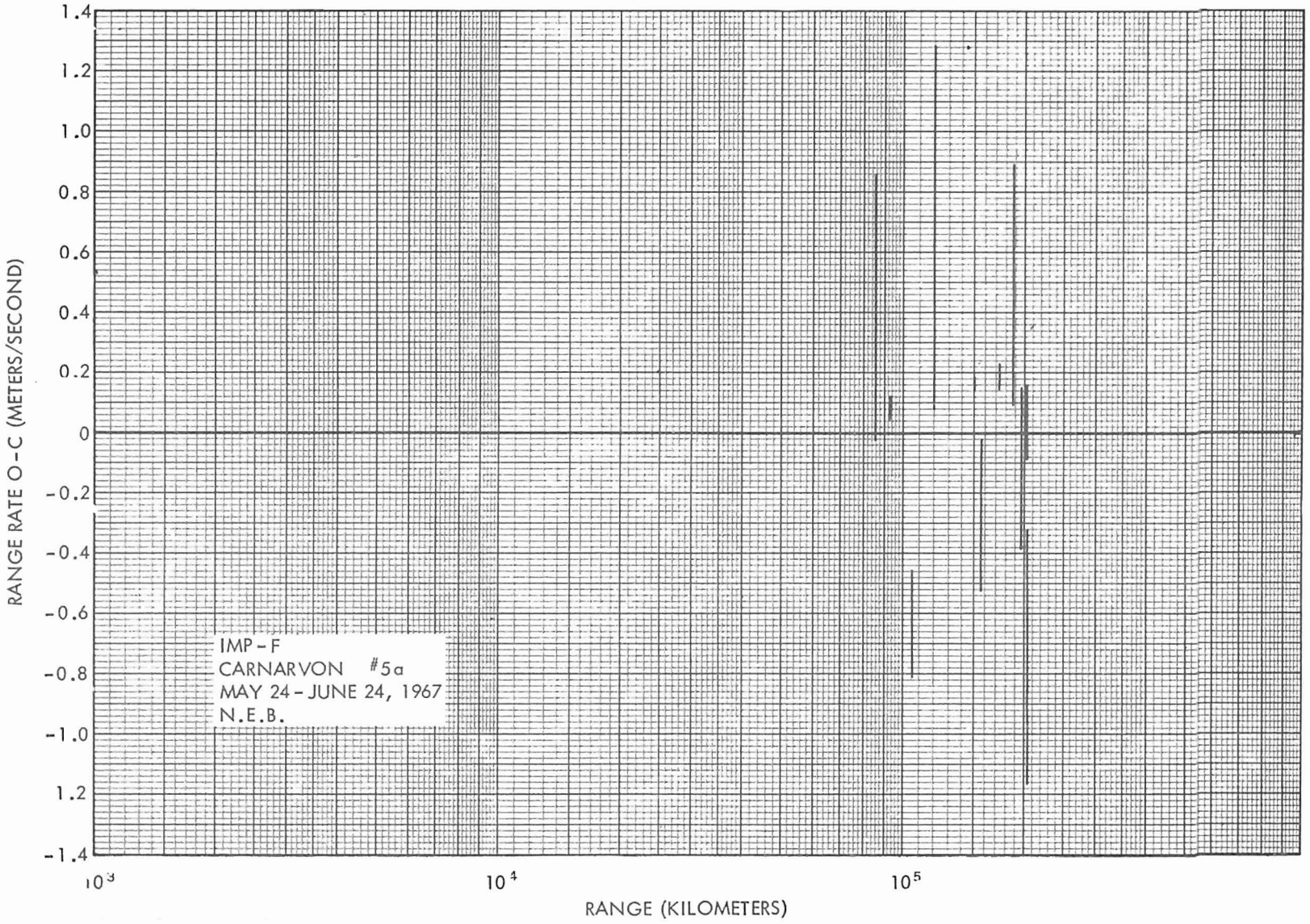
1.4
1.2
1.0
0.8
0.6
0.4
0.2
0
-0.2
-0.4
-0.6
-0.8
-1.0
1.2
-1.4
RANGE RATE O-C (METERS/SECOND)
IMP-F
CARNARVON #5a
MAY 24 - JUNE 24, 1967
N.E.B.
10^3
10^4
10^5
RANGE (KILOMETERS)

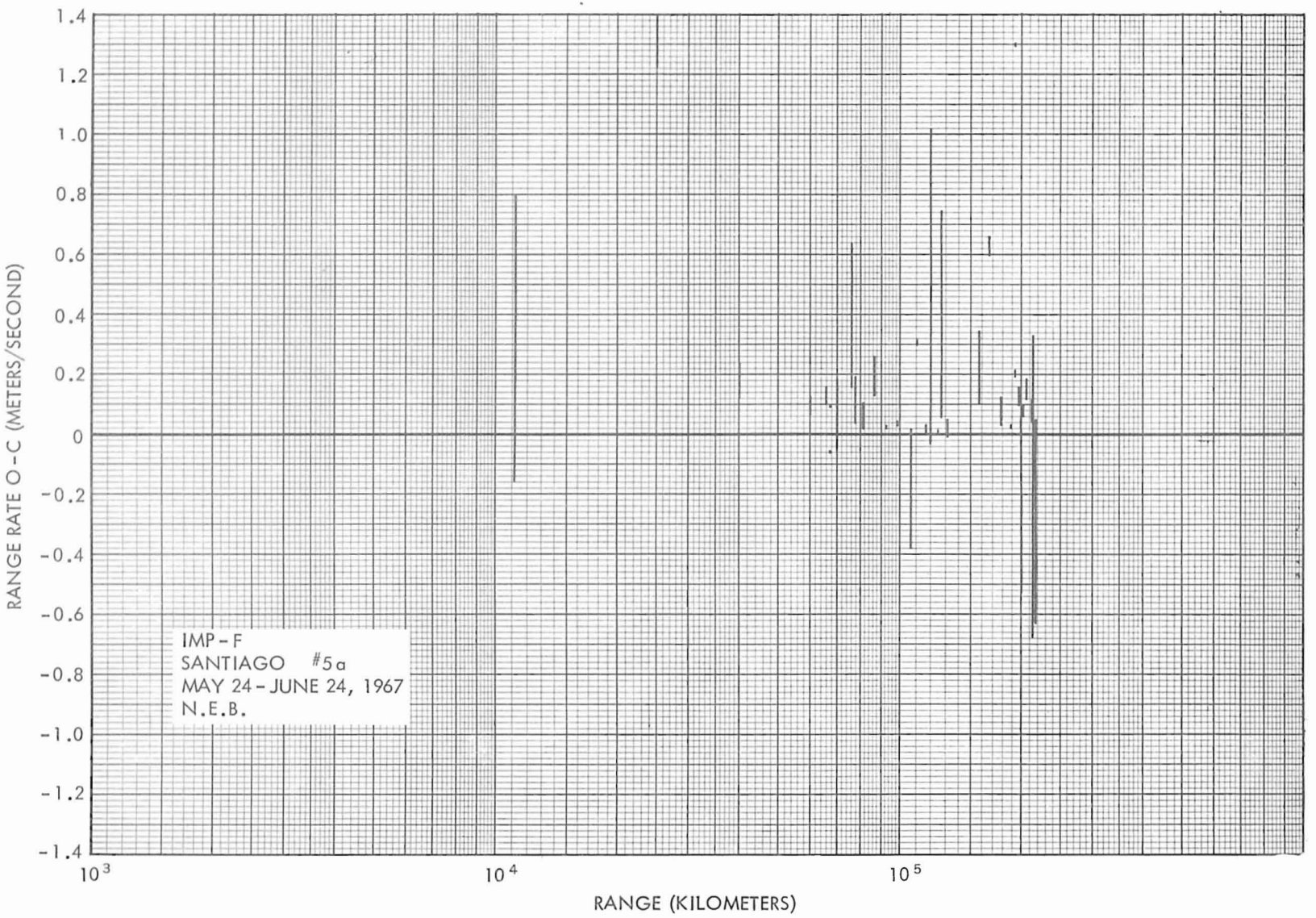
RANGE RATE O-C (METERS/SECOND)
1.4
1.2
1.0
0.8
0.6
0.4
0.2
0
-0.2
-0.4
-0.6
-0.8
-1.0
-1.2
-1.4
10^3
10^4
10^5
RANGE (KILOMETERS)
IMP-F
SANTIAGO #5a
MAY 24 - JUNE 24, 1967
N.E.B.

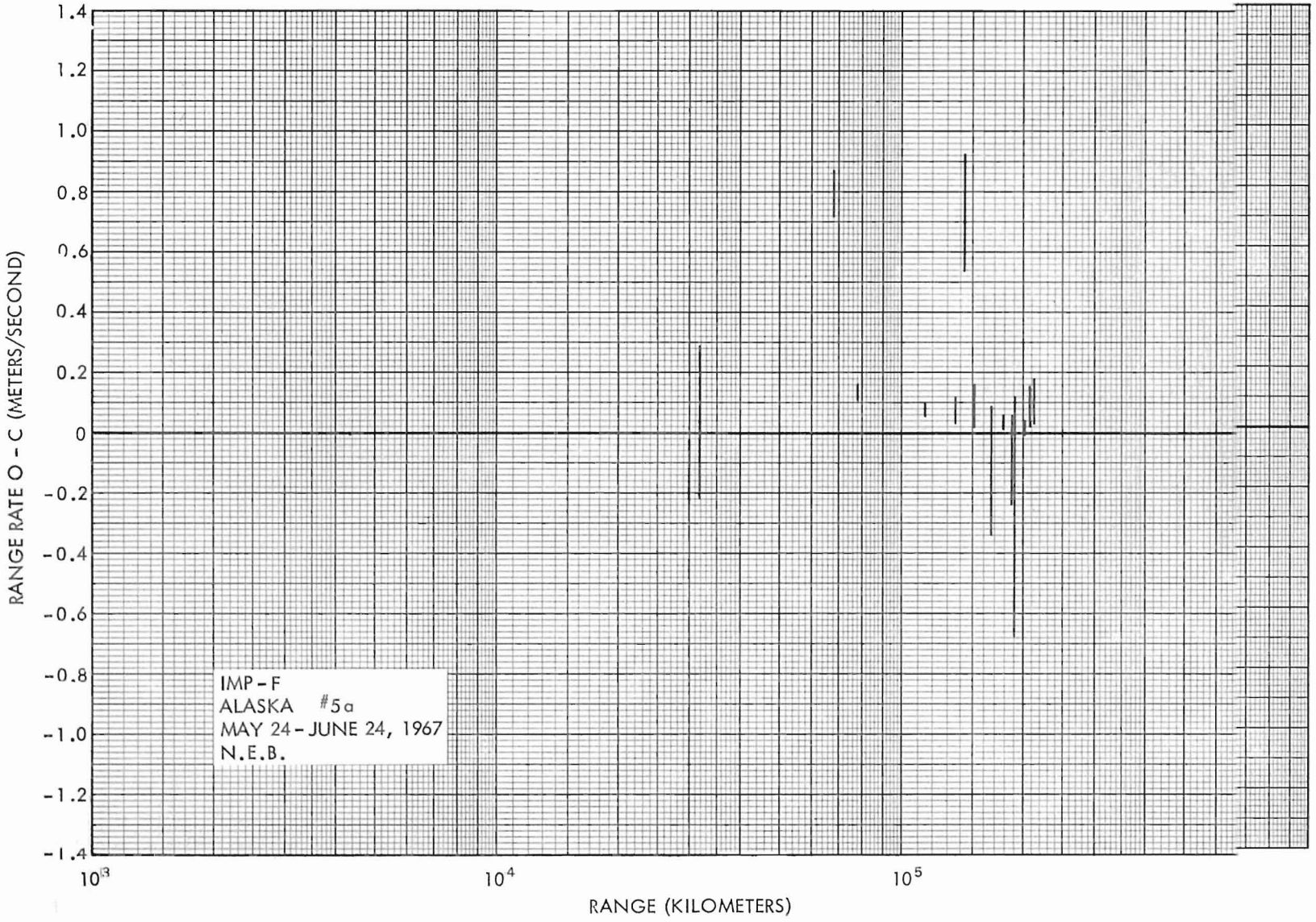
1.4
1.2
1.0
0.8
0.6
0.4
0.2
0
-0.2
-0.4
-0.6
-0.8
-1.0
-1.2
-1.4
RANGE RATE O - C (METERS/SECOND)
IMP - F
ALASKA #5a
MAY 24 - JUNE 24, 1967
N.E.B.
10^3
10^4
10^5
RANGE (KILOMETERS)

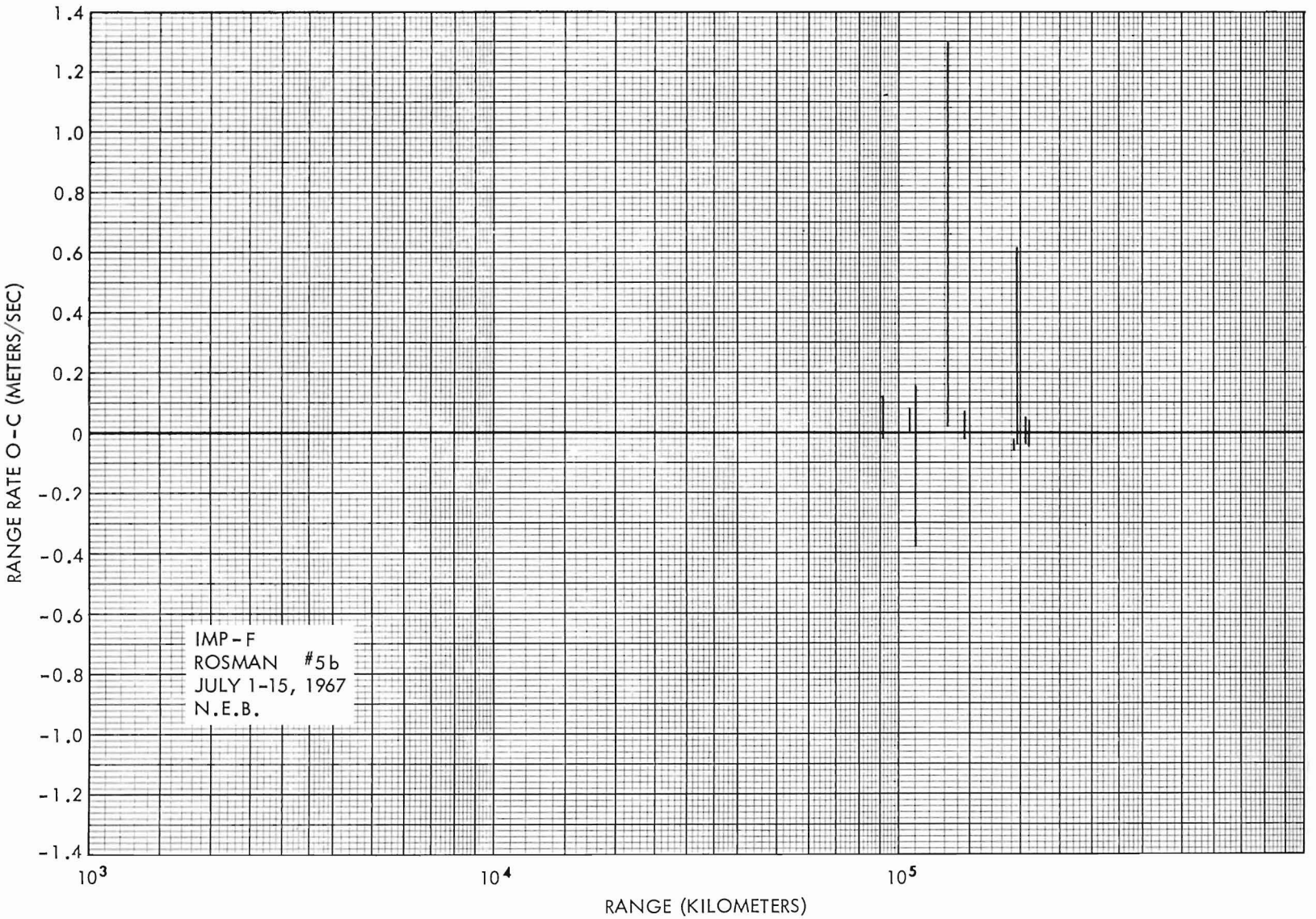
1.4
1.2
1.0
0.8
0.6
0.4
0.2
0
-0.2
-0.4
-0.6
-0.8
-1.0
-1.2
-1.4
RANGE RATE O-C (METERS/SEC)
IMP-F
ROSMAN #5b
JULY 1-15, 1967
N.E.B.
10^3
10^4
10^5
RANGE (KILOMETERS)

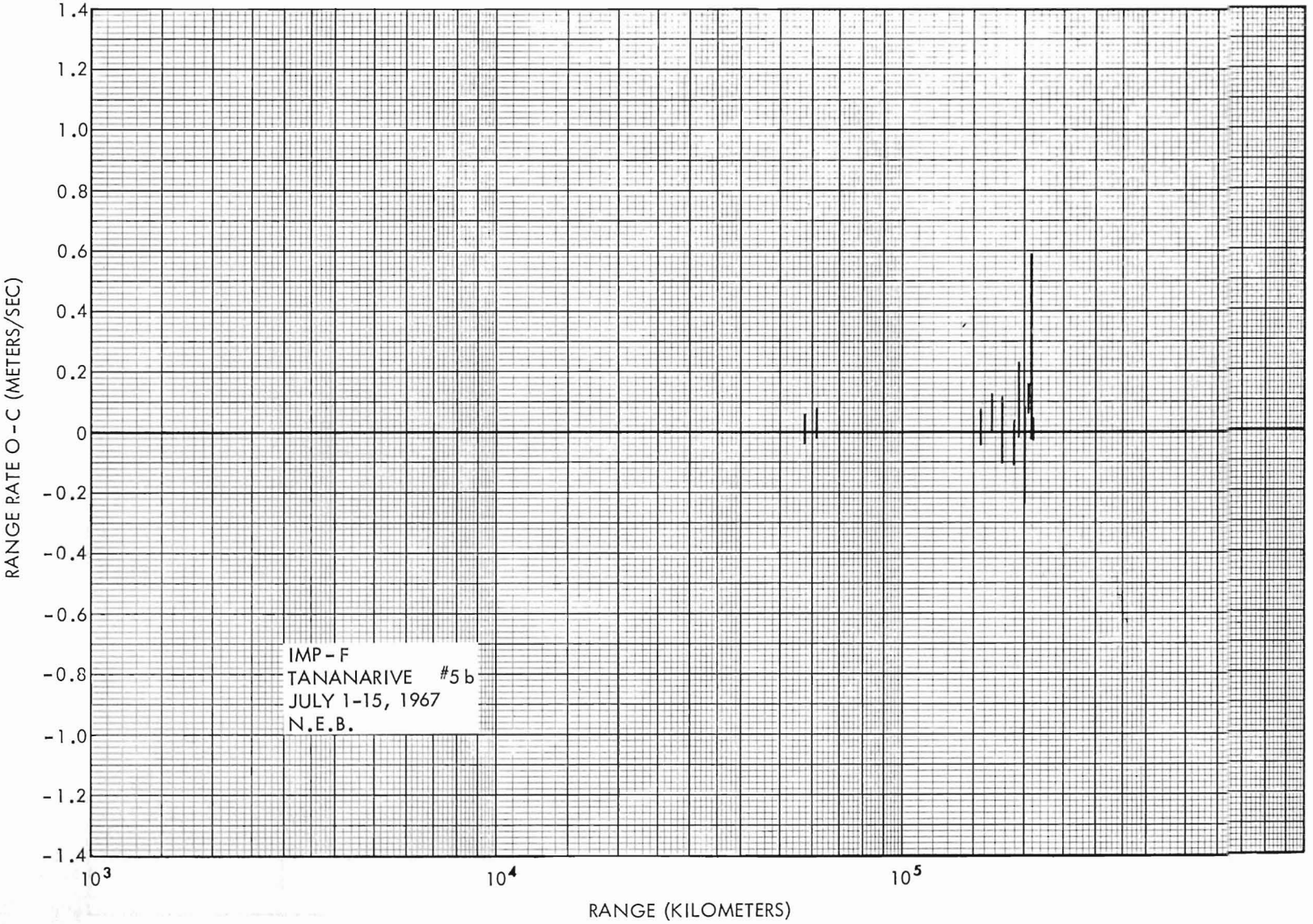
1.4
1.2
1.0
0.8
0.6
0.4
0.2
0
-0.2
-0.4
-0.6
-0.8
-1.0
-1.2
-1.4
RANGE RATE O-C (METERS/SEC)
IMP-F
TANANARIVE #5b
JULY 1-15, 1967
N.E.B.
10^3
10^4
10^5
RANGE (KILOMETERS)

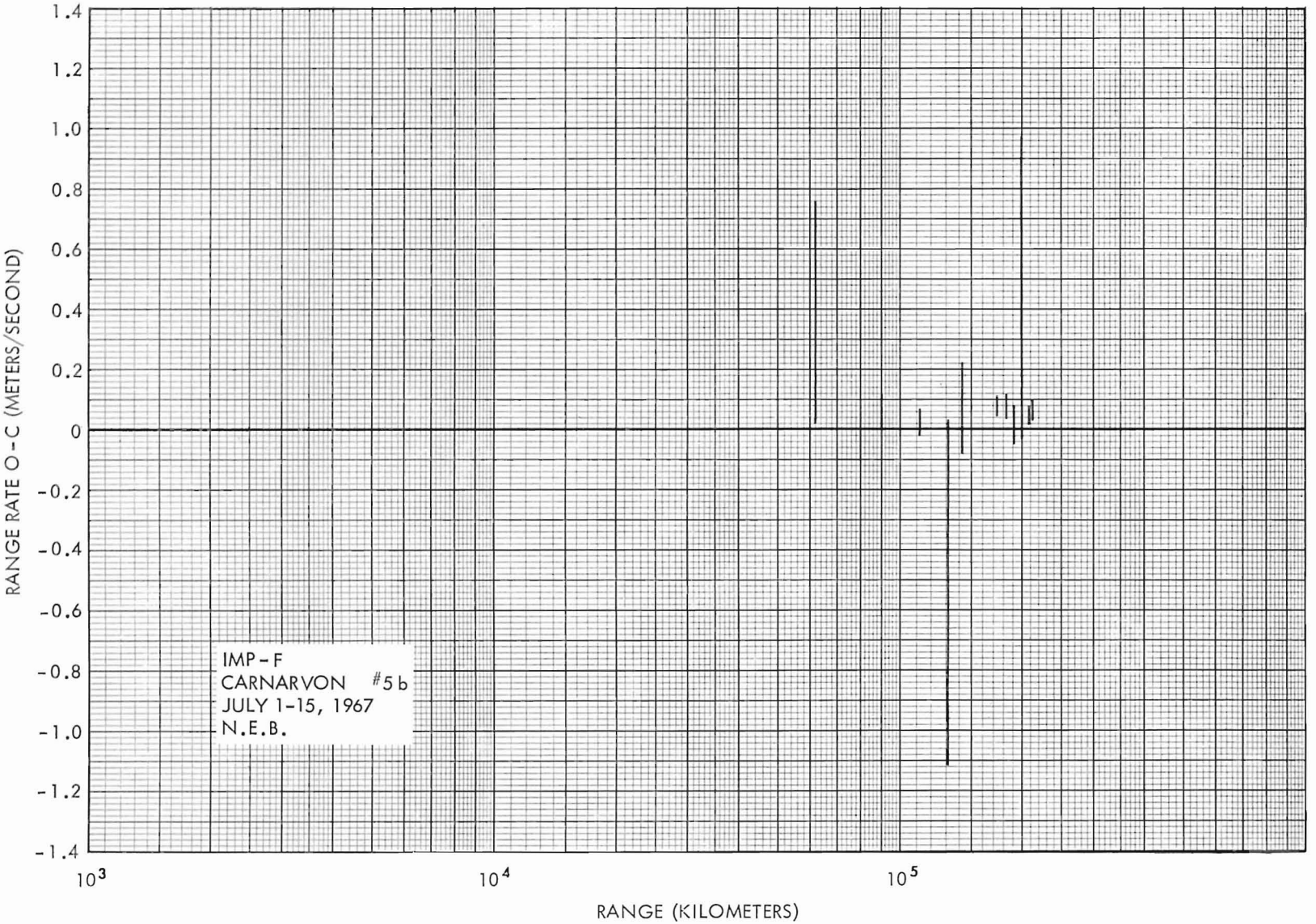
1.4
1.2
1.0
0.8
0.6
0.4
0.2
0
-0.2
-0.4
-0.6
-0.8
-1.0
-1.2
-1.4
RANGE RATE O-C (METERS/SECOND)
10^3
10^4
10^5
RANGE (KILOMETERS)
IMP-F
CARNARVON #5b
JULY 1-15, 1967
N.E.B.

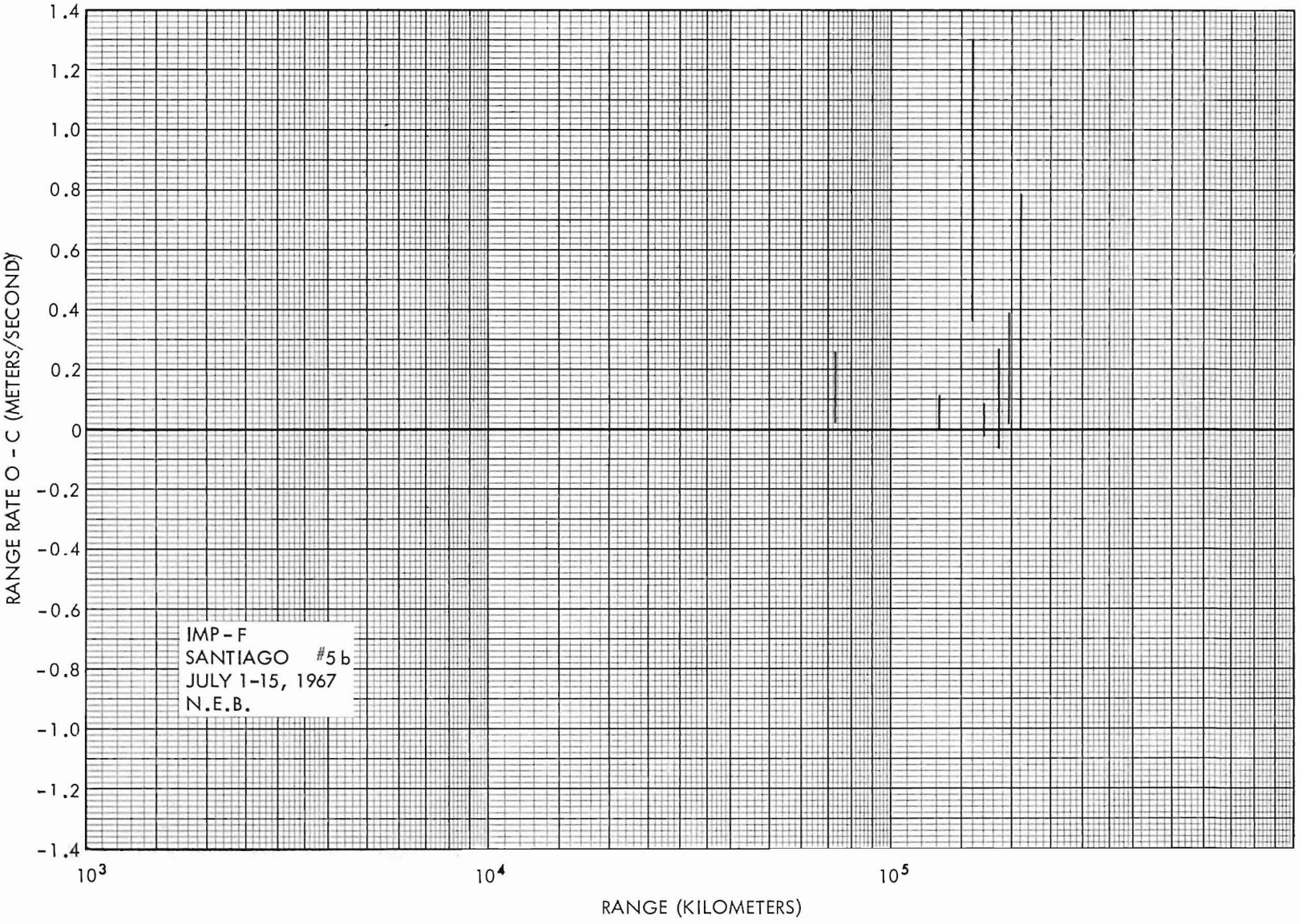
1.4
1.2
1.0
0.8
0.6
0.4
0.2
0
-0.2
-0.4
-0.6
-0.8
-1.0
-1.2
-1.4
RANGE RATE O - C (METERS/SECOND)
IMP-F
SANTIAGO #5b
JULY 1-15, 1967
N.E.B.
10^3
10^4
10^5
RANGE (KILOMETERS)

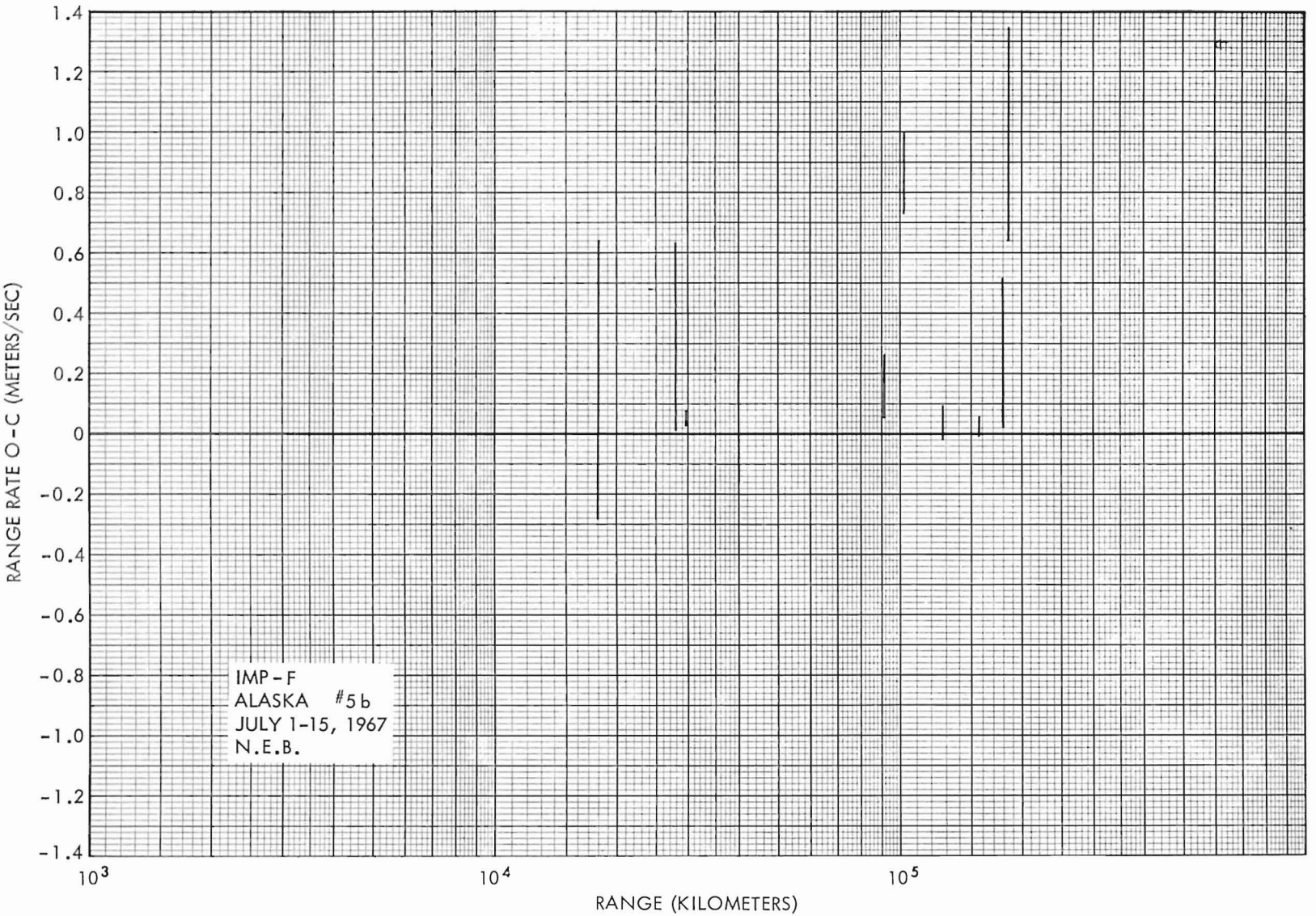
1.4
1.2
1.0
0.8
0.6
0.4
0.2
0
-0.2
-0.4
-0.6
-0.8
-1.0
-1.2
-1.4
RANGE RATE O-C (METERS/SEC)
IMP-F
ALASKA #5b
JULY 1-15, 1967
N.E.B.
10^3
10^4
10^5
RANGE (KILOMETERS)

V. SUMMARY

The GRARR performance in tracking IMP-F is shown rather clearly in the graphs. Most data are well within the minimum expected performance. The minimum expected performance was established in the original system design evaluation report and is based mostly on received signal power and therefore is a good measure for all of the sites even though Alaska and Santiago were built at a later date.

Graph number 1 shows that the signal received at all sites for all ranges is reasonably within the predicted values.

Graph number 2 shows that, at apogee, the noise on the 20 KHz tone exceeded predicted values. Alaska and Santiago show better performance at the extreme ranges primarily because of the additional design effort in the 20 KHz phase locked loop and also because these systems have a sequential mode of operation which provides more signal power in the 20 KHz tone and removes all lower tones after the ambiguity has been resolved.

Graph number 3 shows that the range rate error remained reasonably well within bounds.

Graphs number 4a and 4b show the effect of drag, which is hard for the computer to compensate for, on the range o-c. It is seen that in 4a the o-c is quite large at apogee while in 4b the o-c has been considerably reduced. The results from all sites were fairly consistant.

Graphs number 5a and 5b show the effect of drag on the range rate o-c. It is seen that the effect on range rate was not as significant as on the range o-c.

An overall summary is best shown by Figure 10 which shows an overall RMS range error for the various orbital periods and Figure 11 which shows an overall RMS range rate error. These curves also clearly show the effect of drag during the early life of the spacecraft. As perigee rises, the overall orbital accuracy increases significantly.

In conclusion, it is noted that most data obtained from all sites meet or exceed the minimum expected performance. These data from the GRARR sites have resulted in a knowledge of the IMP-F orbit to within 400 meters RMS in range and 0.1 meters per second RMS in range rate.

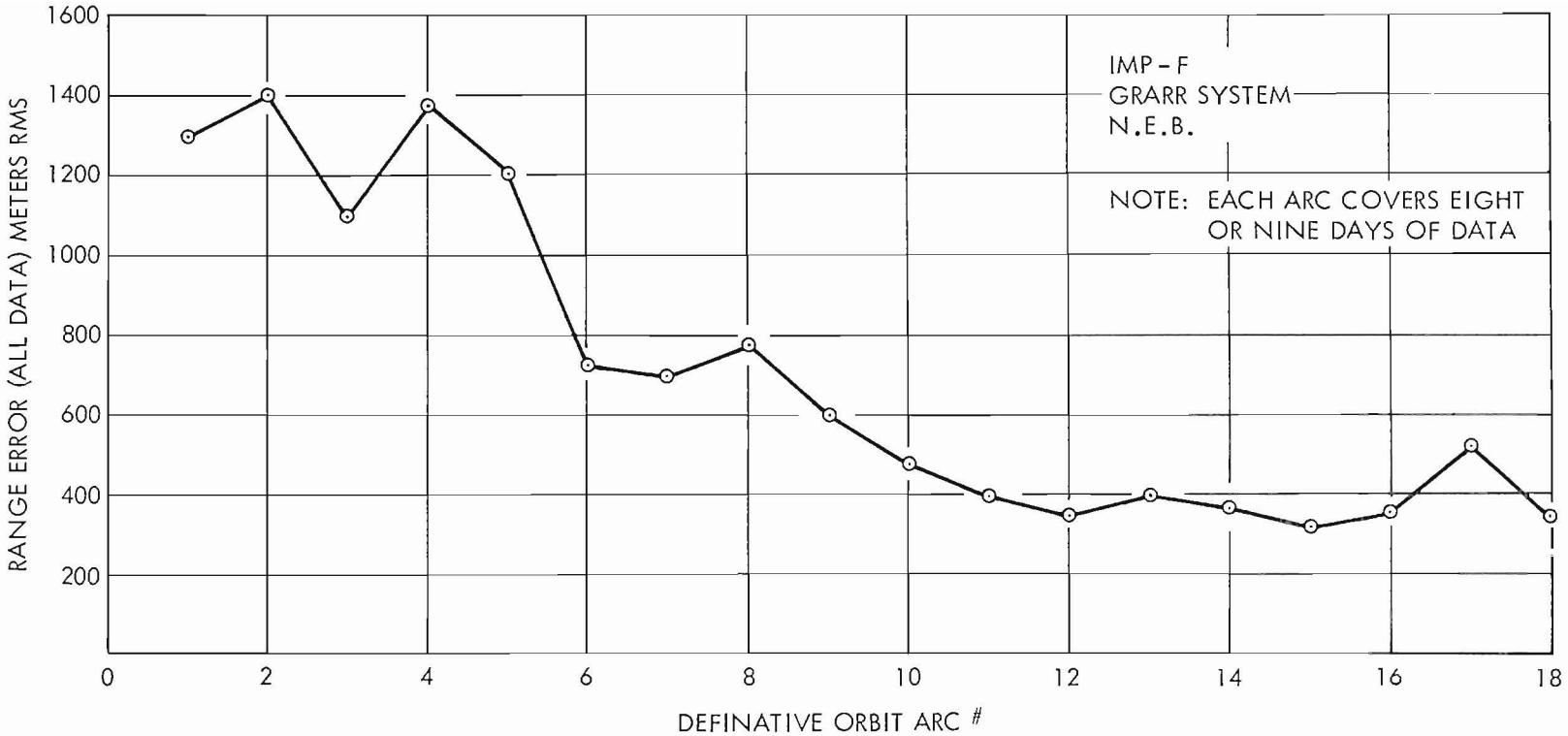
IMP - F
GRARR SYSTEM
N.E.B.
NOTE: EACH ARC COVERS EIGHT OR NINE DAYS OF DATA
RANGE ERROR (ALL DATA) METERS RMS
1600
1400
1200
1000
800
600
400
200
0
2
4
6
8
10
12
14
16
18
DEFINATIVE ORBIT ARC #

Figure 10.

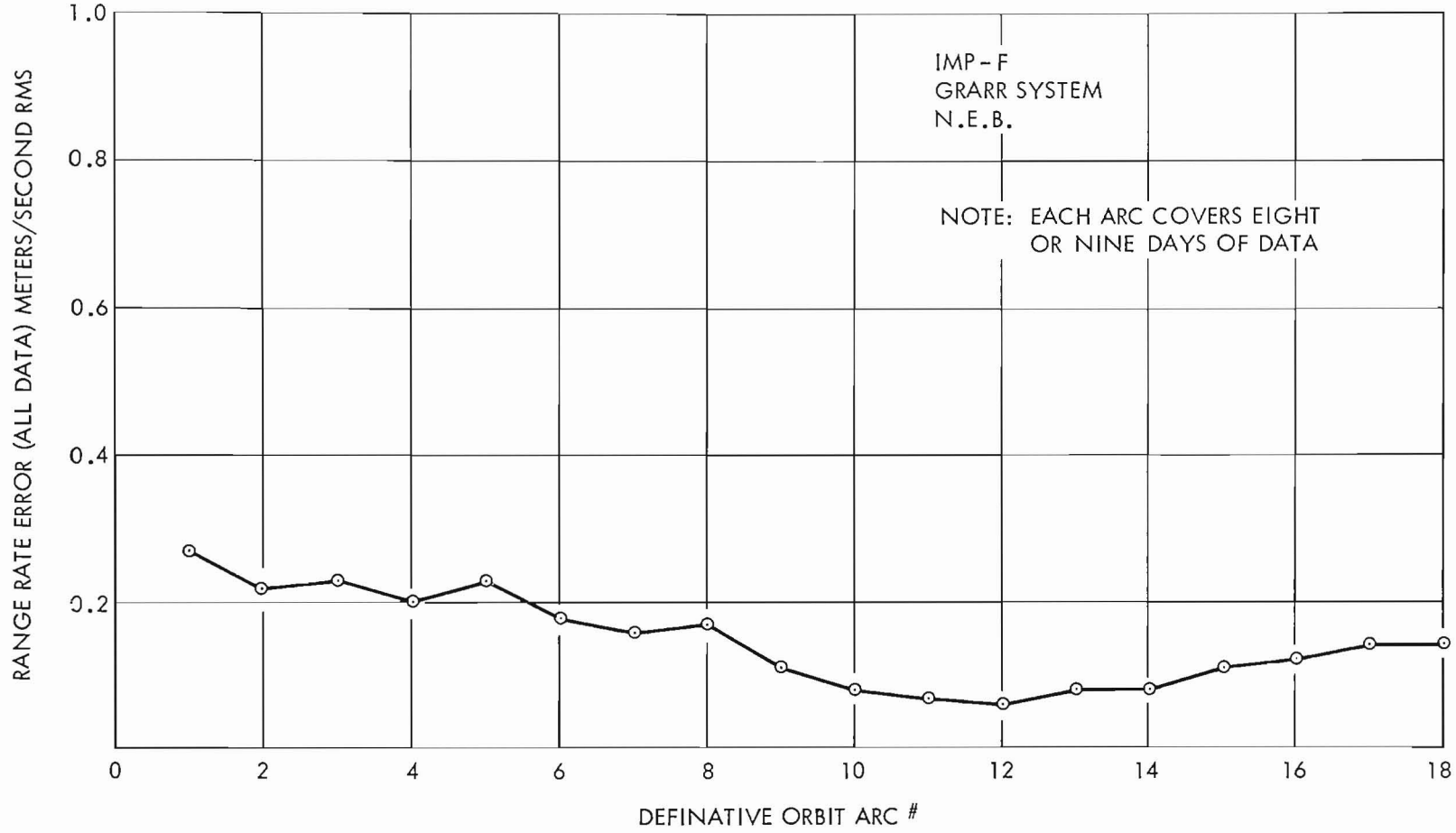
IMP-F
GRARR SYSTEM
N.E.B.
NOTE: EACH ARC COVERS EIGHT
OR NINE DAYS OF DATA
RANGE RATE ERROR (ALL DATA) METERS/SECOND RMS
1.0
0.8
0.6
0.4
0.2
0
2
4
6
8
10
12
14
16
18
DEFINATIVE ORBIT ARC #

Figure 11.

VI. ACKNOWLEDGMENTS

Data gathered for this report represent the results of a team effort between the GRARR Project staff, the system manufacturers, the system operators, and the Data Systems Division. Therefore, the authors wish to acknowledge the efforts of the GRARR site personnel at Rosman, Tananarive, Carnarvon, Alaska and Santiago and thank them for a job well done. The authors also wish to acknowledge the efforts of the Data Systems Division and especially the Theory and Analysis Office for the assistance with the data reduction and the orbital information. Further, it is felt that the design and development efforts of Motorola, Aerospace Center in producing the sites at Rosman, Tananarive and Carnarvon and the General Electric Company, Special Information Products Department in producing the sites at Alaska and Santiago desire special mention because of the excellent system performance.

VII. REFERENCE DOCUMENTS

1. X531-65-403 (NASA GSFC) — The Goddard Range and Range Rate Tracking System; Concept, Design, and Performance, by G. C. Kronmiller, Jr., and E. J. Baghdady. October 1965.

2. X530-67-160 (NASA GSFC) — GRARR Power Spectrum, Threshold Analysis, and Spectrum Diagrams. April 1967.

3. X531-64-71 (NASA GSFC) — A Hybrid Ranging System for Spacecraft, by Fitzgerald, Engels, Shaffer, Habib, Mitchko. April 1964.

4. GSFC — Operation and Maintenance Manual, 0-29, Digital Range Tone Extractor, December 1965.

5. GSFC — Operation and Maintenance Manual, Digital Rate Aid.

6. Motorola Report No. W2719-2-1 — Goddard Range and Range Rate System Design Evaluation Report. November 1962. Contract No. NAS5-1926.

7. Motorola Report No. W2719-29-1 — Test Evaluation Report for Goddard Range and Range Rate System. August 1, 1964. Contract No. NAS5-1926.

8. Motorola Handbook MH-1016 Goddard Range and Range Rate System. July 1, 1964.

9. General Electric — Goddard Range and Range Rate (GRR-2) Design Evaluation Report. November 1964. Contract No. NAS5-9731 and addendum thereto.

10. General Electric — Final Progress Report for the Goddard Range and Range Rate System - Contract NAS5-9731.

11. General Electric Technical Manuals 23-14, Goddard Range and Range Rate System (GRARR). February 23, 1967.

12. General Dynamics, Electronics Division — VHF Transponder Simulator Design Evaluation Report.